International Journal of Hydrogen Energy 266 (2026) 156933

Contents lists available at ScienceDirect

International Journal of Hydrogen Energy

journal homepage: www.elsevier.com/locate/he

Quantifying natural hydrogen prospectivity in Italy: A novel pre-exploration workflow for the energy transition

G. Schirripa Spagnolo [a,*], I. Baneschi [b], A. Rielli [b], A. Billi [c], A.C. Ogunyele [b], L. Aldega [a], M. Lelli [b], A. Caracausi [d], L. Smeraglia [c], G.M. Riolo [d], A. Correale [d], E. Carminati [a], C. Boschi [b,**]

[a] Department of Earth Science, Sapienza University of Rome, Rome, Italy
[b] Institute of Geosciences and Earth Resources, CNR, Pisa, Italy
[c] Institute of Environmental Geology and Geoengineering, CNR, Rome, Italy
[d] National Institute of Geophysics and Volcanology (INGV), Palermo, Italy

A R T I C L E I N F O

Keywords:
H_2 prospectivity index
Pre-exploration workflow
GIS dataset
Ultramafic, intrusive, and organic-rich rocks
H_2 emissions
Energy transition

A B S T R A C T

This study presents the first quantitative evaluation of natural hydrogen prospectivity in Italy, developed within the EU-funded NHEAT—Natural Hydrogen for Energy trAnsiTion—project. It integrates geological, geochemical, and geophysical data through a reaction-specific workflow, and introduces a semi-quantitative hydrogen prospectivity index to classify and rank potential exploration target areas, primarily based on source rocks. The results identify Tuscany as the top-priority region, where granitoid-hosted hydrothermal systems are associated with documented H_2 emissions. The Voltri Massif shows moderate potential linked to active serpentinization, while the Northern Apennines may potentially preserve fossil H_2. In the Ivrea–Verbano Zone, granitoids of Calabria and Sardinia, and in the Western and Central Alps, H_2 could be generated from low-temperature secondary oxidation reactions. The Po Basin may sustain organic-related H_2 production. This national-scale assessment highlights Italy as a natural laboratory for diverse hydrogen systems and provides a transferable workflow for identifying and developing natural hydrogen resources worldwide.

1. Introduction

The energy transition, driven by the dual imperative of mitigating climate change and strengthening energy security, demands the rapid deployment of low-emission technologies and diversification of clean energy sources. European and national strategies, such as the *European Green Deal* [1] and the *REPowerEU Plan* [2], identify hydrogen as a key energy carrier. However, current roadmaps focus almost exclusively on green hydrogen despite limitations related to renewable power availability, water resources, and production costs [3,4]. In contrast, natural hydrogen, also known as white, native, or geological hydrogen, forms spontaneously in the Earth's subsurface, offering low extraction costs, zero direct CO_2 emissions, and compatibility with existing energy infrastructures [5–7]. Despite these advantages, its potential remains poorly explored and is mostly absent from current energy transition strategies (Fig. 1).

Several abiotic reactions in the Earth's crust and upper mantle generate H_2, with a global flux estimated at roughly 40 to >64 Mt y^{-1} [9]. After formation, natural H_2 can migrate by advection along high-permeability structural pathways until it is effectively trapped beneath very low-permeability seals such as salt, anhydrite, and clay [10,11]. H_2 losses from reservoirs may occur via molecular diffusion driven by concentration gradients, advective leakage along dry or water-saturated fractures, or consumption by biotic and abiotic reactions [12–14]. Large uncertainties remain regarding subsurface H_2 residence times [9,14], but a global mass-balance model by Ellis & Gelman [11] suggests that approximately 5.6×10^6 Mt of H_2 may be preserved in the subsurface over geological timescales. A few accidental discoveries of economically significant subsurface H_2 accumulations, such as those in Mali and Albania [15,16], demonstrate that substantial concentrations can indeed be preserved and exploited. These examples emphasize the necessity of systematic, geology-based exploration

* Corresponding author.
** Corresponding author.
E-mail addresses: giulia.schirripaspagnolo@uniroma1.it (G. Schirripa Spagnolo), chiara.boschi@cnr.it (C. Boschi).

https://doi.org/10.1016/j.ijhydene.2026.156933
Received 12 November 2025; Received in revised form 30 April 2026; Accepted 4 August 2026
Available online 12 August 2026

strategies to identify hydrogen-prone settings rather than relying on chance discoveries.

To address this challenge, several pre-exploration workflows have been proposed to integrate geological, geophysical, and geochemical datasets for mapping H_2-favorable areas. Early frameworks by Moretti et al. [17] and Lévy et al. [18] outlined basin-scale screening criteria based on reactive lithologies and surface gas evidence, delivering systematic but largely qualitative approaches. Building on these foundations, Donzé et al. [19] developed a probabilistic model calibrated on the Bulqizë massif (Albania), combining geothermal, magnetic, and hydrogeochemical indicators of serpentinization. Despite this methodological advance, the applicability of that model remains limited to ophiolitic contexts.

As a key novelty, this study, primarily focused on H_2-generating mechanisms, extends the probabilistic framework of Donzé et al. [19] to a broader range of geological settings, including thermogenic degradation of organic matter and hydrothermal alteration of Fe-rich igneous rocks. In the proposed approach, indicators of H_2 genesis are divided into two categories: conditions and evidence. Greater weight is assigned to conditions, as they are essential for H_2 production—most fundamentally, the presence of source rocks at depth. By contrast, direct and indirect evidence (e.g., shallow H_2 emissions) may be absent even where subsurface accumulations exist. The model also introduces the distinction between active and fossil serpentinization, reflecting the different conditions required for the formation and preservation of H_2 accumulations in these two cases.

This framework introduces an H_2 Prospectivity Index coupled with a data completeness factor, providing the guidance for efficient exploration planning that identifies where additional data collection is needed and where exploration efforts should be prioritized. The approach is tested using Italy as a case study, where the geological setting is favorable for multiple H_2 generation processes—and yet a comprehensive, national-scale evaluation of H_2 prospectivity is still lacking. Developed within the NHEAT project of national relevance (PRIN PNRR 2022), this

Fig. 1. The role and value chain of natural hydrogen in the energy transition (modified after [8]). The figure illustrates processes capable of generating H_2 in significant quantities and their integration within the broader hydrogen value chain.

study supports national-scale evaluations of natural H_2 potential and the identification of high-priority exploration targets. Our reaction-specific workflow model, based on reproducible and editable matrix-based computations, can be easily applied to other geological contexts or H_2-generating mechanisms. Since the framework mainly focuses on generation-related indicators, it can be readily updated as new geological information and refined criteria for H_2 accumulation and preservation—processes that remain only partially constrained in the literature—become available, thereby progressively improving the identification of hydrogen-prospective targets.

2. Potential natural hydrogen source in Italy

Several natural processes are known to generate H_2, including serpentinization, hydrothermal alteration of Fe-rich igneous rocks, oxidation of Fe-rich sedimentary rocks such as banded iron formations (BIFs) and siderite deposits, thermal decomposition of organic matter, mantle degassing, magmatic activity, fracture-induced reduction of water, and radiolysis [20–26]. These processes are, however, highly site-specific, and their local significance depends on the presence, abundance, and spatial distribution of suitable reactive lithologies. A detailed understanding of the lithological framework is therefore essential to reliably assess the potential of H_2 generation in a given area. Italy lacks extensive iron-rich sedimentary rocks such as BIFs and siderite deposits, although minor Fe-rich deposits may contribute marginally (e.g., Ref. [27,28]). Likewise, H_2 generated by radiolysis of water is not considered in this work, as it is typically associated with U-, Th-, and K-bearing minerals hosted in Archean–Proterozoic terranes, which are absent in Italy [21,25,29,30]. Nonetheless, radioactive elements occur in accessory phases such as zircon, apatite, and monazite within the Tuscan and Calabrian granites [31–33] and in U-bearing ores related to hydrothermal alteration of Upper Carboniferous-Lower Permian acidic volcanic rocks in the Southern Alps [34]. Furthermore, U-bearing lignites are exposed in Central Italy and Sardinia, where radioactive decay could cause radiolysis of organic matter [35]. Although these deposits contain appreciable U_3O_8 concentrations [34,35], their relatively young age suggests a negligible contribution to H_2 generation. The Italian geological framework is characterized by widespread ophiolitic complexes, geothermal and volcanic systems, abundant granitoid intrusions, and sedimentary basins. Within this context, such lithological and structural settings would be expected to host processes including serpentinization, hydrothermal alteration of Fe-rich igneous rocks, organic matter degradation, and, to a lesser extent, volcanic activity (Table 1), all recognized as potential sources of H_2.

Serpentinization is the reaction of ultramafic rocks with water that forms serpentine, magnetite, and occasional brucite, while releasing H_2, CH_4, and hyperalkaline fluids [46–49]. H_2 is generated through the reduction of water coupled with the oxidation of Fe^{2+} in olivine and orthopyroxene [22,36,50,51]. Serpentinization proceeds most effectively under hydrothermal conditions (150–300°C) typical of oceanic lithosphere, but it also occurs in continental environments such as ophiolitic massifs, orogenic peridotites, and Archean greenstone belts [10,16,37,52]. Similarly, the interaction between hydrothermal fluids and other Fe^{2+}-bearing minerals, such as amphiboles (e.g., arfvedsonite, riebeckite) and biotite, can generate H_2 through oxidation of ferrous iron and formation of magnetite at rates comparable to those of serpentinization [38–40]. A related process is hematitization, defined as the low-temperature (<150°C) oxidation of magnetite to hematite (α-Fe_2O_3), which can occur in both hydrothermally altered granites and serpentinites [41,53]. In addition, the thermal cracking of overmature organic matter within coalfields or organic-rich shales can generate H_2, whereas microbial processes such as fermentation and nitrogen fixation may also contribute, although most biologically produced H_2 is typically consumed by concurrent microbial reactions [42,43,54]. Finally, mantle-derived H_2 associated with volcanic activity, or produced through the reduction of magmatic gases such as H_2S and SO_2, may be locally significant in Italy due to the presence of active volcanic systems [44,45]. However, the technical and regulatory challenges of exploring in high-risk volcanic zones (e.g., Campania, Lazio, Sicily) currently limit their exploitation potential. The following sections therefore focus on the aforementioned H_2-generating processes, excluding those related to volcanic activity, starting from the characterization of the rocks and the corresponding geological and geochemical settings in which these processes occur.

3. Italian geological and geochemical setting

After identifying the processes most relevant to H_2 production in Italy, the geological, tectonic, and magmatic evolution of the region is summarized to assess their influence on the subsurface generation, migration, accumulation, and preservation of natural H_2. The present-day structural, geological, and magmatic framework of Italy results from the convergence between the European and Adriatic-African plates during the Alpine orogeny (Mesozoic–Present), superimposed on the older Hercynian one [55,56]. The subduction and collision stages of the Alpine cycle led to the closure of the Alpine Tethys Ocean, the opening of the Tyrrhenian back-arc basin, and the buildup of the Alps and the Apennines orogens (Fig. 2). This long-lived orogenic evolution produced a strongly heterogeneous lithosphere, in which (ultra)mafic, granitoid, sedimentary, and volcanic rocks of different ages coexist and are affected by a dense network of faults and active geothermal-magmatic processes (Fig. 2b). Such lithological and structural heterogeneity

Table 1
Principal natural hydrogen generation processes and their relevance in Italy.

Process	Main reactions	Typical H_2 yield	Occurrence in Italy	Exploration relevance	Key references
Serpentinization	Olivine/pyroxene + H_2O → serpentine + magnetite + H_2 (150–300°C)	High (up to thousands of ppmv)	Ophiolitic complexes (both in the Alps and Apennines)	High	[22,36,37]
Hydrothermal alteration of Fe-rich rocks	Alteration of Fe^{2+} minerals (biotite, amphibole) → Fe^{3+} phases + H_2	Moderate to high	Granitoid intrusions, geothermal fields (Tuscany, Sardinia)	High	[38,39] [40];
BIF oxidation/ hematization	Magnetite → hematite + H_2	Low to moderate	Minor Fe-rich deposits (local occurrences)	Low	[27,41]
Thermogenic or microbial degradation	Thermal cracking or fermentation of organic matter	Moderate to high	Po Plain, Apennine foredeep basins, coalfields in Sardinia	Moderate	[14,42,43]
Radiolysis of water or organic matter	α, β, γ decay of U–Th–K minerals → H_2 + oxidants	Moderate to high	Accessory U–Th–K minerals in Tuscany and Calabria. U-bearing ores in Southern Alps (Novazza and Val Vedello) and in Sardinia	Low	[29,30,34,35]
Volcanic/mantle degassing	Reduction of H_2S, SO_2 in magmatic gases or direct mantle release	Variable, locally high	Active volcanic areas (Campania, Lazio, Sicily)	Low — limited by technical and regulatory constraints	[44,45]

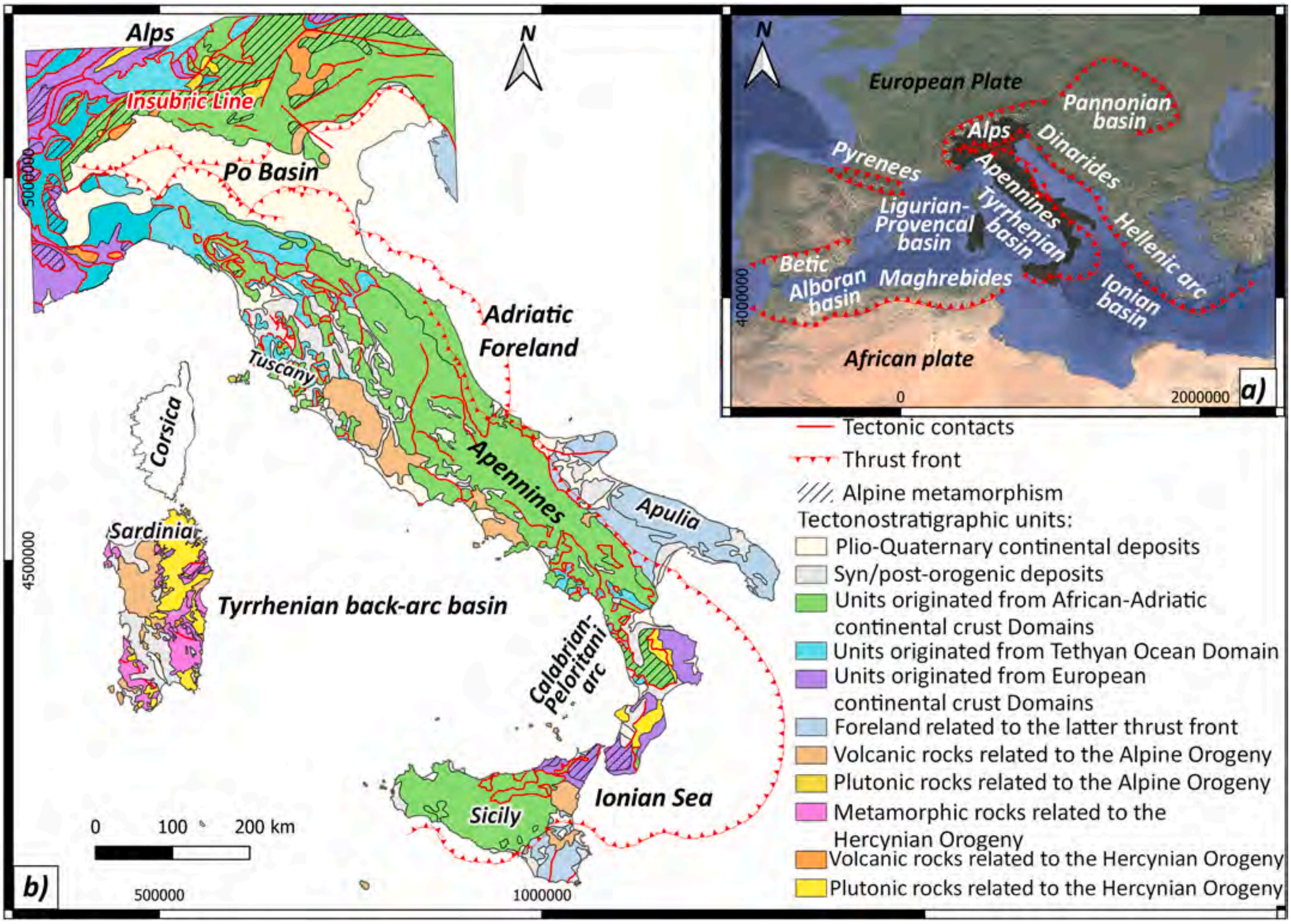

Fig. 2. a) The map of the Mediterranean area showing the main orogenic belts, basins, and subduction zones. The study area shown on panel b is marked in black. b) Map of the tectonostratigraphic units of Italy (WGS84/UTM 32 N; modified by "Carta Geostrutturale dell'Italia 1:1000000" of ISPRA [57].

exerts a primary control on potential H_2 systems because it governs both the sources of H_2 (e.g., rock types prone to H_2-producing reactions) and the pathways and traps for H_2 migration and accumulation. In this framework, mafic and ultramafic rocks that are capable of producing H_2 through serpentinization in Italy include ophiolitic bodies derived from the Tethys Ocean, mainly exposed in the Western–Central Alps and in the Northern-Central Apennines (Fig. 2b). In the Apennines, serpentinite bodies are generally weakly metamorphosed or unmetamorphosed [49, 58–61], whereas they often record high-pressure metamorphism in the Alpine belt ([62,63]; Fig. 2b). Igneous rocks rich in Fe-bearing minerals, formed during both Hercynian and Alpine orogenic cycles, represent an additional potential source of H_2. Intrusive rocks include Hercynian granitoids widely exposed in the Eastern and Southern Alps that, in some cases, underwent Alpine metamorphism [64]. Hercynian granitoids also occur in Sardinia and Calabria [65,66]. Younger magmatism, associated with the Alpine subduction, emplaced tonalite-granodiorite intrusions mainly along the Insubric Line (Fig. 2b), between 32 and 28 Ma [67,68]. In Tuscany, subduction-related granitoid intrusions, associated with Tyrrhenian back-arc crustal thinning, occurred between 8 and 1 Ma [69–71]. Concerning volcanic rocks, late Paleozoic acidic volcanics, related to late Hercynian stages, crop out mainly in the Alps [72]. Instead, volcanic rocks exposed in Sardinia, Sicily, and the Apennines are related to Alpine magmatism ([45,68,73]; Fig. 2b) and range from basaltic to more alkaline compositions. Alpine-cycle magmatism is still active in southern and central Italy and is expressed by high-temperature fluid manifestations, such as volcanic plumes, fumaroles, and boiling pools where intense CO_2 fluxes ($\sim 2.1 \times 10^{11}$ mol/y; [74,75]) are accompanied by CH_4, N_2, and noble gases [76,77]. Although H_2 is typically a minor constituent of the dry gas fraction (<0.1 vol%), localized enrichments have been documented in the Larderello geothermal area (2.5-6.4 vol%; [78,79]) and near active volcanic centres such as the Solfatara (1.25 vol%; [80]), Ischia (up to 4.2 vol%; [81]), Vesuvio (1.2 vol%; [82]), and Pantelleria (13 vol%; [83]; Table S2). In Italy, natural gas emissions are not limited to magmatic and hydrothermal provinces: cold gas emissions from soils, vents, or aquifers are widespread in non-volcanic settings [84,85]. These manifestations are multi-component systems, where H_2 is either absent or present only in trace amounts (Tables S1–S2). For instance, gas discharges along the Apennine thrust front are dominated by CH_4-rich fluids of thermogenic or microbial origin [86,87], whereas those in Sardinia consist of CO_2–N_2 or CO_2-CH_4 mixtures. In both cases, H_2 contents are negligible (<0.04 vol% [85,88,89]; and references within; Table S2), likely due to oxidation and dilution with other carrier phases.

Gas-geochemical datasets are most comprehensive in Central-Southern Italy ([85], and references therein), owing to the volcanic monitoring activities, and in Tuscany [78,79,84,90–92] due to geothermal exploration. Conversely, in other regions, particularly in the Northern Apennines and the Alps, fluid geochemical information remains more limited and spatially localized ([93–99]; Table S2). This uneven coverage limits our ability to assess the national distribution of H_2 occurrences and to evaluate resource potential at basin and regional scales. Nevertheless, the Italian geological framework hosts multiple, physically plausible sources and reservoirs for H_2, which warrant detailed investigation in the following sections.

4. Integrated workflow

The proposed workflow combines geological, geochemical, and geophysical data with spatial analysis and semi-quantitative weighted scoring to identify areas with potential for natural H_2 generation and preservation across Italy. Considering the selected H_2-generating reactions, the workflow consists of three main steps.

(i) integration of geological, geochemical, and geophysical datasets within a GIS framework,
(ii) identification of evidence and condition indicators for each H_2-generating processes, and
(iii) semi-quantitative estimation of H_2 prospectivity to prioritize exploration targets.

4.1. Step 1: data compilation and GIS-based integration

Geological, geochemical, and geophysical data were integrated into QGIS to build thematic maps correlating rock types, structural trends, geothermal conditions, and gas-emission data. Geological inputs, such as rock and fault mapping, are derived from the Geological Map of Italy (1:1,000,000 scale; ISPRA [57]) and from the Structural Model of Italy (1:500,000 scale; MASE [100]). Building on the previous identification of the most relevant H_2-generating processes for the Italian context (Table 1), we select the associated potential hydrogen generation rocks (H_2-GR; modified after [18]).

- H_2-GR1: mafic and ultramafic rocks (peridotites, serpentinites, gabbros, and basalts), capable of generating H_2 through the water-rock interaction involving Fe^{2+}-bearing minerals (active or fossil serpentinization);
- H_2-GR2: Fe-rich igneous rocks (granitoids and rhyolites) potentially affected by hydrothermal alteration;
- H_2-GR3: organic-rich sedimentary rocks, where thermogenic degradation of the organic matter may produce H_2.

We exported and examined polygon attribute tables of H_2-GR1 and H_2-GR2 in QGIS software to determine their areal extension across the Italian territory. For H_2-GR3 rocks, we used locations of productive hydrocarbon wells from the MASE database [101] as proxies for potential subsurface H_2 co-generation. The second GIS layer includes locations where H_2 has been detected in near-surface soil gases [93,99], in the dry fraction of gas emissions (e.g., mofettes and fumaroles), and in dissolved gas of springs and wells ([84,85], and references therein), supplemented with updated records from Gherardi et al. [92], Leila et al. [78], Granieri et al. [79], de Freitas et al. [99], and the unpublished National Institute of Geophysics and Volcanology (INGV) database (see Tables S1 and S2). Regarding geophysical data, we integrated the Earth Magnetic Anomaly Grid (EMAG2v3; [102]) and mapped surface heat-flow contours derived from the geothermal map of Della Vedova et al. [103], available through the GeothermCatalog of the Institute of Geosciences and Earth Resources, National Research Council of Italy (IGG-CNR).

4.2. Step 2: reaction-specific evidence and condition indicators

For each selected process, specific indicators—evidence and conditions—were identified to reflect the distinct geological and geochemical signatures of different H_2-generating processes (Table 2), based on an extensive review of the literature. Table 2 illustrates that some indicators are common to all processes, whereas others are specific to individual mechanisms. For serpentinization, fossil and active systems are distinguished because they are characterized by different indicators. The most critical one is the target source rock type and its degree of serpentinization: peridotites or peridotites with low grades (<20%) of serpentinization containing olivine, which could generate H_2 nowadays in active systems, versus highly (>70%) or fully serpentinized rocks, which could have produced substantial quantities of H_2 in the past, now potentially preserved in the subsurface, in fossil systems. In areas where both peridotites and highly serpentinized rocks are present, a unique classification is not possible; therefore, H_2 prospectivity is evaluated considering both active and fossil systems.

We define evidence as direct or indirect indicators supporting H_2 production (e.g., reactive lithologies, H_2 and CH_4 anomalies, alkaline springs, etc.). The absence of such evidence does not necessarily exclude the possibility of a subsurface reservoir. Conditions, instead, correspond to geological, thermal, and geochemical prerequisites for, primarily, H_2 formation (e.g., presence of target rock at depth, adequate heat flow, etc.; Table 2) and, secondarily, its preservation (favorable structural architectures for H_2 accumulation and preservation; Table 2).

4.3. Step 3: semi-quantitative calculation of H_2 prospectivity index

To translate the conceptual framework defined in Section 4.2 into a reproducible analytical tool for identifying the most promising areas for potential future H_2 exploration, we implement a semi-quantitative approach, fully described in Appendix A.

In the first step, we separately quantify the evidence and condition

Table 2
Evidence and conditions for active and fossil systems, such as serpentinization, and for active hydrothermalism and thermogenic degradation of organic matter. "✓" indicates applicable and "n/a" not applicable indicators.

	Serpentinization (active)	Serpentinization (fossil)	Hydrothermalism	Degradation of organic matter
Evidence				
Target rock exposure at the surface	✓	✓	✓	n/a
Alkaline springs indicating ongoing water–rock reactions	✓	n/a	✓	n/a
CH_4 emissions as proxy of ongoing serpentinization	✓	n/a	n/a	n/a
H_2 emissions as a potential indicator of seepage from a deep resource	✓	✓	✓	✓
H_2 trapped in fluid inclusions indicating fossil H_2 generation	n/a	✓	n/a	n/a
Hydrocarbon wells indicating the occurrence of kerogen at depth	n/a	n/a	n/a	✓
Magnetic anomalies consistent with serpentinite bodies at depth.	n/a	✓	n/a	n/a
Conditions				
Target rocks at depth (from geophysical data or geological interpretations)	✓	✓	✓	✓
Volume estimates (reactive mass available)	✓	✓	✓	n/a
High heat flow supporting reaction kinetics	✓	n/a	✓	n/a
Total Organic Compounds (TOC, wt%)	n/a	n/a	n/a	✓
Thermal maturity of kerogen expressed as vitrinite reflectance (R_o %)	n/a	n/a	n/a	✓
Favorable structural architecture (reservoir rocks, sealing horizons). In the fossil system it also includes the tectonic history	✓	✓	✓	✓

scores (E and C) for each investigated area (see equation (1) in Appendix A). These scores are calculated as normalized weighted averages of the values (Vi) assigned to each indicator applicable to the selected H_2-generating process (defined by the indicator flag Fi) in the study area. The weights (Wi) assigned to each indicator reflect its relative geological importance within the H_2-generating processes (see Tables A.1 and S3, *Ranking Criteria*). To account for heterogeneous data coverage, completeness factors (CF_e and CF_c) were introduced as the ratio of the evidence or conditions available for the study area to the total number of evidence or conditions applicable to the investigated process (see equation (2) in Appendix A). Previous parameters (E and C, CF_e and CF_c) are then summed using the α weight (see Appendix A) to obtain the score and completeness factor of all indicators (i.e., I and CF; see equations (3) and (4) in Appendix A).

At this point, the H_2 Prospectivity Index (H_2_index) is computed as the product of I, CF, and Tr (see equation (5) in Appendix A), where Tr is a binary geological filter for target rock at depth (Tr = 0 when potential source rocks are absent, resulting in a null index; Tr = 1 where they are present; see Table S3). The resulting E, C, CF, and H_2_index values for all investigated areas are reported in Table S3 and used to classify hydrogen prospectivity into four classes: > 0.75 = High; 0.50–0.75 = Moderate; 0.25–0.50 = Low; < 0.25 = Very Low/Uncertain.

The product of I, CF, and Tr (see Equation (5) in Appendix A), where Tr is a binary geological filter for target rocks at depth (Tr = 0 when potential source rocks are absent, resulting in a null index; Tr = 1 when they are present).

Sensitivity tests, performed by varying the adopted weights (α and Wi) across all H_2-generation processes and selected areas, demonstrate the stability of the highest-prospectivity regions and thus confirm the robustness of the proposed semi-quantitative approach (see Appendix A and Table S3). Table S3 reports all input values (indicator list, Wi, Vi), intermediate results (E, C, I, CF), final scores (H_2_index), and sensitivity tests facilitating reproducibility and enabling application of the model to other geological settings or H_2-generating mechanisms.

4.4. *H_2 production and energetic basis of the volumetric threshold*

The H_2 generation and energy assessment provides the quantitative basis for a volumetric threshold that will be adopted for our ranking criteria of the semi-quantitative framework, directly constraining the potential scale and economic significance of natural H_2 systems (Appendix A). The volume of reactive lithologies is the main control on H_2 yield. Stoichiometric estimates indicate that, theoretically, a 100 km^3 peridotite body with 10% FeO could generate ~310 Mt H_2 if fully serpentinized. Similarly, a 100 km^3 biotite-rich granite could yield 85–120 Mt of H_2 depending on the oxidation state of biotite (see Appendix B for details; [39,104]). Assuming complete reaction and full gas retention, these values correspond to 14–38 EJ (≈3900–10, 500 TWh) of energy, equivalent to 2–6% of current global annual energy demand ([3]; see Appendix C for energy conversion assumptions).

Under more realistic—though still optimistic—conditions (10–80% reaction progress; 10% trapping efficiency; strongly inhibited biotic/abiotic consumption; [11]), the amount of recoverable H_2 is preliminarily estimated to range from 3 to 25 Mt for peridotites and 1 to 10 Mt for granitic systems (Appendix B). To relate geological potential to economic feasibility—and in line with the targets of the European Hydrogen Strategy (10 Mt H_2 yr^{-1} by 2030)—a reference volumetric threshold of 100 km^3 of reactive rock was adopted (Appendix B; Fig. 3). This volume corresponds to a theoretical sustainable H_2 production (≥0.5 Mt H_2 yr^{-1}) over an operational lifetime of about 20 years, a scale that is considered sufficient to justify capital investment and ensure long-term economic feasibility [105,106]. Given the uncertainties associated with several processes (reaction progress, trapping efficiency, and preservation), this threshold should be regarded as a first-order screening based on geological criteria for identifying areas where hydrogen production may be economically significant. To evaluate and guarantee the presence of a recoverable resource, more detailed, site-specific analyses will subsequently be required.

4.5. *Method limitations*

The main limitation of the proposed approach lies in the fact that the selection of indicators, the associated threshold, and the Wi assignment are based on the still limited understanding of natural hydrogen systems, particularly with respect to migration pathways, trapping efficiency, and preservation potential. In addition, only a few natural hydrogen reservoirs have been identified worldwide to date, which limits the calibration of the model across all H_2-generating processes. These

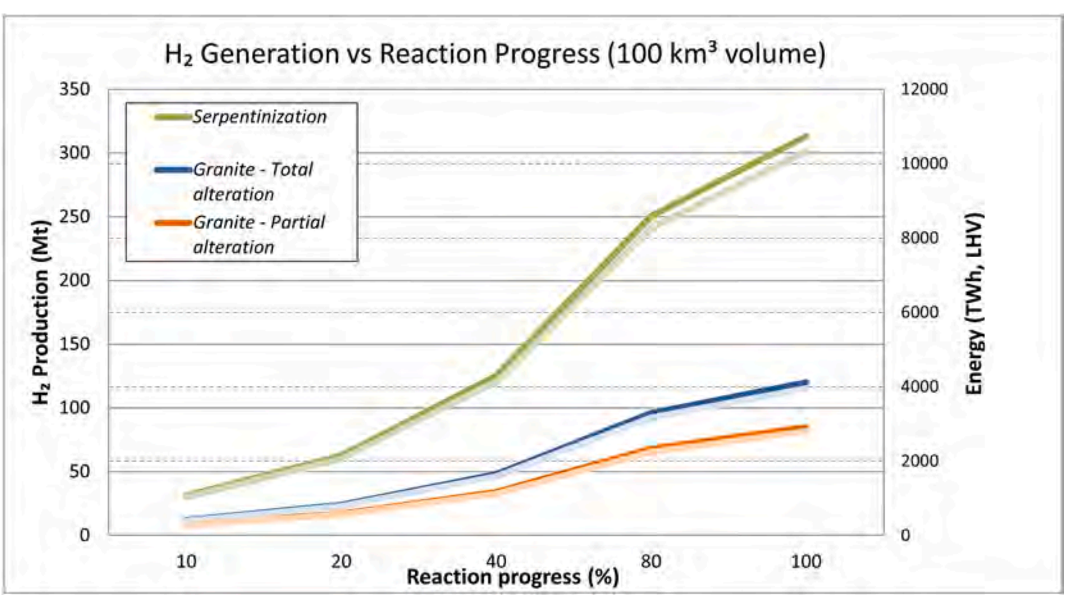

Fig. 3. Molecular h*ydrogen generation potential as a function of reaction progress for a* 100 km^3 *rock volume.* Dark lines represent H_2 production (Mt), whereas lighter lines indicate the corresponding equivalent energy yield (TWh, LHV). Serpentinization (green) produces up to three times more H_2 than granite alteration (blue = total; orange = partial) under comparable reaction progress. H_2 estimates were derived from stoichiometric calculations using compositional data from Leong et al. [104] and Murray et al. [39]. (For interpretation of the references to colour in this figure legend, the reader is referred to the Web version of this article.)

aspects should therefore be considered when interpreting the results.

Despite these limitations and the present inability to reliably predict subsurface H_2 accumulations, the proposed approach provides a practical framework for identifying areas where additional data collection is needed to improve hydrogen prospectivity assessment, for prioritizing exploration targets, and for supporting reservoir discovery efforts.

5. Italian hydrogen potential: results and discussion

Mafic–ultramafic (H_2-GR1) and Fe-rich igneous rocks (H_2-GR2) are the primary H_2-generating lithologies in Italy, together covering approximately 10% of the national surface area (Fig. 4). Mafic–ultramafic rocks (H_2-GR1) include both Tethyan-derived ophiolites (serpentinites, gabbros, basalts, eclogites, and peridotites) and basaltic lavas. Ophiolites are discontinuously preserved along the Italian peninsula, in the Western Alps (~1300 km^2), Central Alps (~300 km^2),

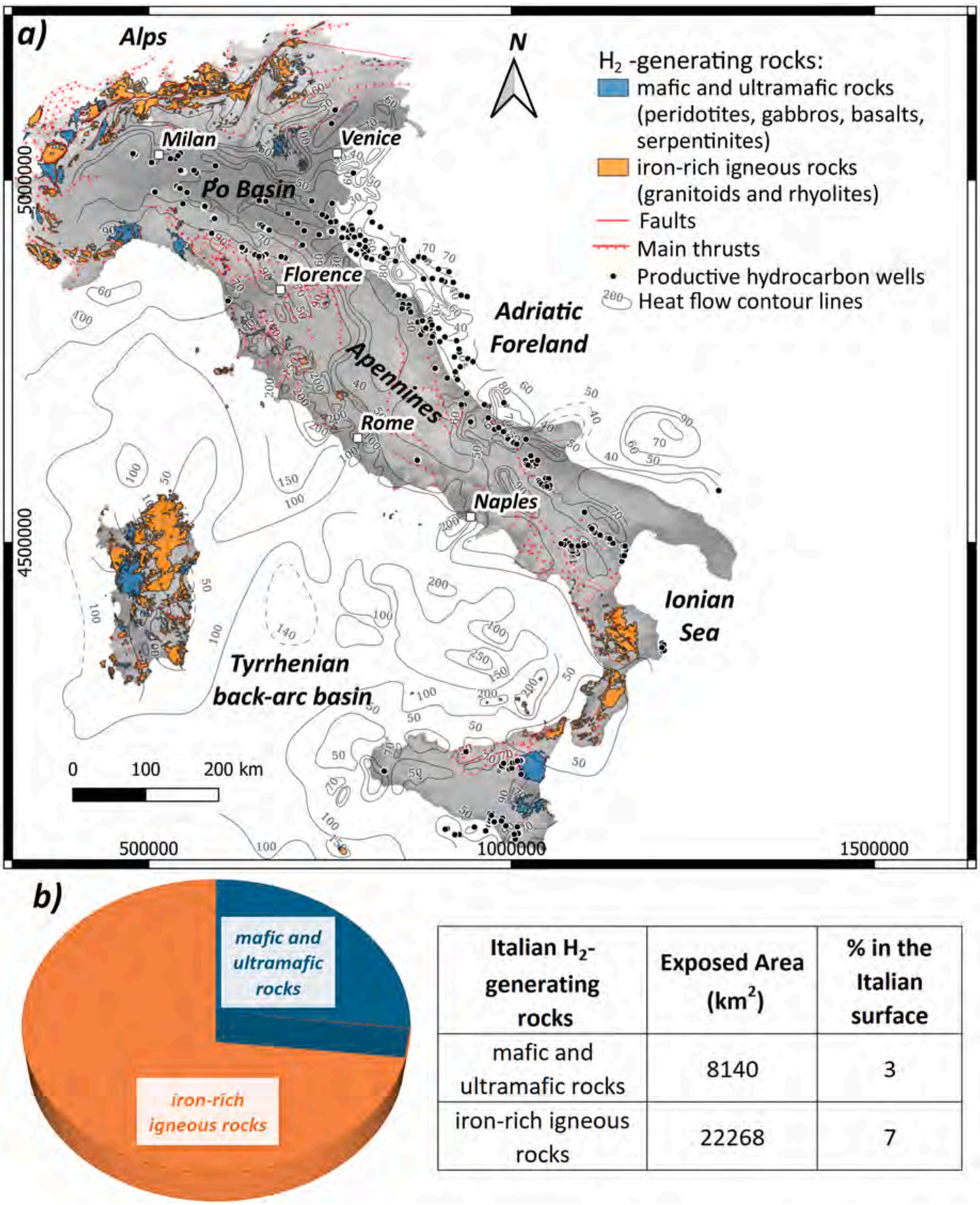

Italian H_2-generating rocks	Exposed Area (km^2)	% in the Italian surface
mafic and ultramafic rocks	8140	3
iron-rich igneous rocks	22268	7

Fig. 4. a) The map of H_2-generating rocks in Italy (WGS84/UTM 32 N) with also the locations of hydrocarbon productive wells (MASE database; [101]) and surface heat flow (mW/m^2) contour lines by Della Vedova et al. [103]. b) Pie chart of Italian H_2-generating rocks with their superficial areas (km^2) and their percentage coverage of the Italian territory.

Ligurian Alps (~700 km^2), Northern Apennines (Liguria, Emilia, and Tuscany regions, ~800 km^2), and Southern Apennines (Calabria region, ~150 km^2). Instead, basaltic lavas are mainly exposed in Sardinia (~1700 km^2), Sicily (~1800 km^2), and the Eastern Alps (~500 km^2). Collectively, these units cover approximately 8000 km^2, corresponding to about 3% of the Italian territory. Fe-rich mafic lithologies such as gabbros and basalts, although not directly involved in serpentinization, may contribute to H_2 generation through oxidation of Fe-bearing minerals, a process that can occur alongside serpentinization.

Fe-rich igneous rocks (H_2-GR2), including granites, metagranites, and peralkaline rhyolites, are mainly exposed in the Alps, Sardinia, and the Calabrian arc, covering an overall area of about 22,000 km^2, equivalent to 7% of the Italian surface. Particularly Fe-enriched peralkaline rhyolites (pantellerites) occur on Pantelleria Island [107], where the highest H_2 concentrations in Italy have been measured (up to 13 vol%; Table S2). However, since regions with exposed rhyolites coincide with high-risk volcanic areas, where both technical and regulatory constraints severely limit exploitation, they are excluded from the following discussions.

5.1. Active serpentinization

5.1.1. Evidence

Fresh peridotites are widely exposed in the Lanzo (~80 km^2) and Voltri (~110 km^2) massifs (Table 3; Fig. 5). The Lanzo Massif is a large ultramafic body (~150 km^2) with a peridotite core composed mainly of lherzolite and, subordinately, harzburgite and dunite, surrounded by a serpentinized shell (Bourdier et al., 1978; [112,113]). The Voltri Massif, instead, hosts meter-to kilometer-scale discontinuous bodies of peridotite within strongly foliated serpentinites (e.g., Ref. [114]). Minor exposed peridotite bodies are also preserved in the Ivrea Verbano Zone (IVZ; ~30 km^2; Table 3) and in the Ligurian-Emilian Apennines (~50 km^2; [19,110,112,115]). Notably, these peridotite bodies host podiform or layered chromitites (in the IVZ) and Cr-rich spinel (in the Emilian Apennines), which may act as catalysts for H_2 generation [19,110].

Several alkaline and hyperalkaline springs were documented in the Voltri Massif, where they are associated with ultramafic rocks ([94,95,97,98,116,117]; Fig. 5). H_2 and CH_4 were documented in hyperalkaline springs both in the Voltri Massif [95] and the Northern Apennines ([99]; Figs. 5 and 6; Table 3). The $\delta^{13}C$ and δ^2H isotopic signatures of CH_4 dissolved in these springs indicate an abiotic origin [95,99], providing additional evidence of ongoing serpentinization.

The absence of reported alkaline or hyperalkaline springs as well as H_2 emissions in the Lanzo Massif and IVZ likely reflects differences in tectonic evolution and/or depth of serpentinization, or, alternatively, may result from the lack of detailed hydrogeological investigations.

5.1.2. Conditions

The IVZ presents extensive peridotite bodies extending from the surface to depths of 10–15 km, as revealed by recent 3-D seismic and crustal models indicating a tilted ultramafic lens several tens of kilometers long [109,118]. The Lanzo and Voltri Massifs, although lacking dedicated geophysical surveys, likely host significant peridotite volumes at depth, as suggested by interpretative cross-sections showing well-defined ultramafic layers [108]. In the Ligurian Apennines, confined lenses of ophiolites occur at depths of 5–7 km [111], whereas in the Emilian and Tuscan Apennines they are closer to the surface (0.5–1 km; [61,110]). However, the tectono-metamorphic evolution of these regions suggests that these ophiolitic rocks are extensively serpentinized [49,119]. Although advanced serpentinization reduces olivine abundance, relict olivine grains may nevertheless remain reactive and participate in active serpentinization [110].

Ultramafic rocks in the Alps and the Ligurian–Emilian Apennines, though widespread both at the surface and at depth, are associated with low heat flow (<100 mW/m^2) and normal geothermal gradients (~30 °C/km) (Fig. 5; Table 3), limiting serpentinization at shallow levels where optimal temperatures (100–350°C, peak > 200°C; [120–122]) are rarely reached. However, under such low temperature conditions, H_2 could be produced by the ongoing oxidation of Fe^{2+}-bearing secondary minerals within serpentinites, including brucite and magnetite [51].

In contrast, the Tuscan Apennines display much higher heat flow (≥400 mW/m^2) and intense hydrothermal circulation, especially in the Larderello and Monte Amiata geothermal fields (Fig. 5). Despite the limited availability of detailed geophysical data, most ultramafic domains exhibit a favorable structural architecture for H_2 migration and trapping. This is primarily due to the pervasive faulting, which enhances fluid circulation, and the juxtaposition of high- and low-permeability rocks, which promotes fluid accumulation [61,98,108,123].

5.2. Fossil serpentinization

5.2.1. Evidence

Fossil serpentinization refers to ancient hydration of ultramafic rocks, for example, in mid-oceanic ridges or in subduction zones [46,63]. H_2 produced by such processes may be preserved in deep reservoirs where structural and stratigraphic conditions are favorable. In the Alpine domain, both the Lanzo Massif and the Valmalenco—located close to the Insubric Line—include approximately 70 km^2 of exposed serpentinites. Moreover, Aosta Valley and Voltri Massif expose about 225 and 470 km^2, respectively—the largest serpentinite areas in Italy (Table 4). All these rocks in the Alpine domain are characterized by a high degree of serpentinization (60 - 80%; [126,128]) up to full serpentinization in the Voltri Massif [129]. Conversely, the Ivrea–Verbano Zone, although underlain by deep peridotite bodies, has minimal serpentinite outcrops characterized by a very low degree of serpentinization (<20%; [126]). In the Apennines, ultramafic rocks characterized by a strong degree of serpentinization (>70%; [49,59,110]) cover about 110 km^2 in the Ligurian and Emilian regions, over 130 km^2 in Tuscany,

Table 3
Evidence and conditions for active serpentinization in target areas indicating whether each selected area satisfies the ranking criteria defined in the semi-quantitative H_2 Prospectivity Index framework (Appendix A and Table S3).

Target area	Evidence				Conditions				
	Target Rock exposure (Peridotite) (km^2)[1]	H_2 emissions (vol %)	CH_4 emissions (vol %)	Alkaline springs	Target Rocks at depth (Peridotite)	Volume estimates (km^3)	Heat Flow (mW/m^2)[9]	Active magmatic/hydrothermal system	Favorable structural architecture
Lanzo Massif	80	N.d.	N.d.	N.d.	Yes	>100[5]	60	No	Yes
Ivrea-Verbano	30	N.d.	N.d.	N.d.	Yes	>100[6]	70	No	Yes
Voltri Massif	110	< 0.001[2]	16 - 19[2]	Yes[4]	Yes	>100[5]	80	No	Yes
Ligurian-Emilian Apennines	50	<0.002[3]	8.9[3]	Yes[3]	Yes	≪ 100[7,8]	70	No	Yes

N.d. = no data; 1) Structural Model of Italy at scale 1:500,000 ([*100*]; 2) [95]; 3) [99]; 4) [94]; 5) [108]; 6) [109]; 7) [110]; 8) [111]; 9) [103].

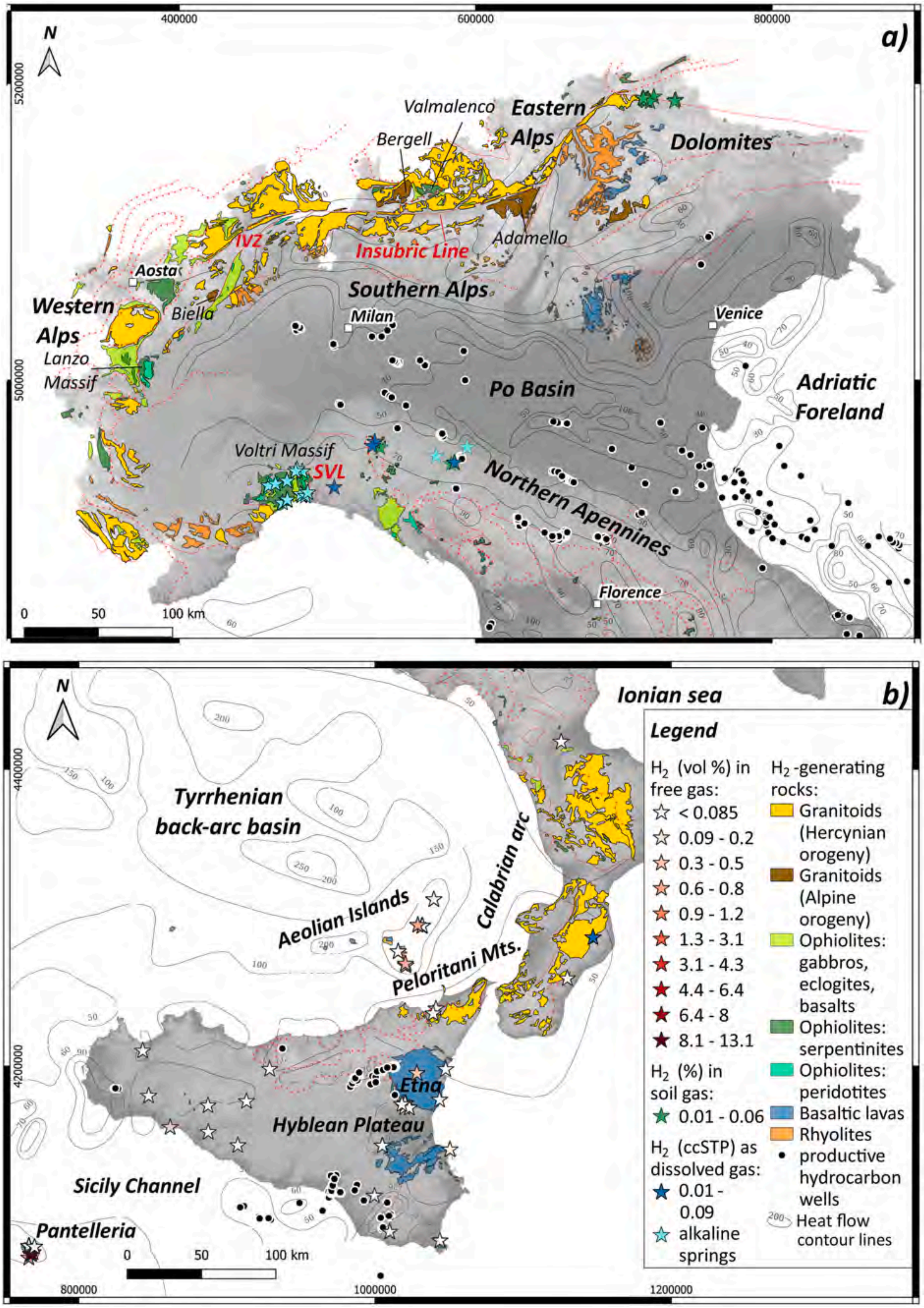

Fig. 5. Maps of Northern (panel a) and Southern Italy (panel b) showing potential H_2-generating rocks and H_2 measurement sites (Tables S1 and S2; [93,99]) (WGS84/UTM 32 N). Maps also include surface heat flow (mW/m^2) contour lines by Della Vedova et al. [103] and the locations of hydrocarbon productive wells (MASE database; [101]).

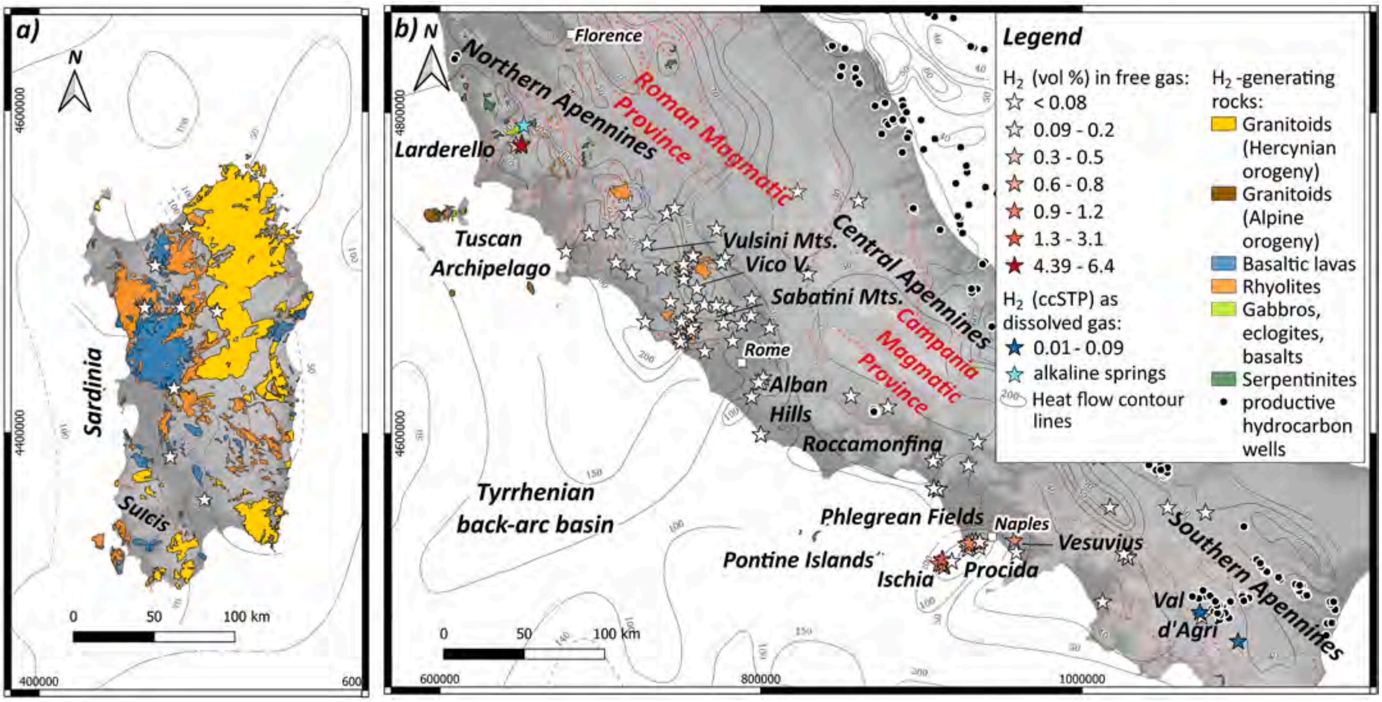

Fig. 6. Maps of Sardinia (panel a) and Central Italy (panel b) showing potential H_2-generating rocks and H_2 measurement sites (Tables S1 and S2; [93,99]) (WGS84/UTM 32 N). Maps also include surface heat flow (mW/m^2) contour lines by Della Vedova et al. [103] and the locations of hydrocarbon productive wells (MASE database; [101]).

Table 4
Evidence and conditions for fossil serpentinization in target areas indicating whether each selected area satisfies the ranking criteria defined in the semi-quantitative H_2 Prospectivity Index framework (Appendix A and Table S3).

Target area	Evidence				Conditions		
	Target rock exposure (Serpentinite) (km^2)[1]	H_2 emissions (vol %)	H_2 in fluid inclusions	Magnetic anomalies (nT)[9]	Target rock at depth (Serpentinites)	Volume estimates (km^3)	Favorable structural architecture
Lanzo Massif	70	N.d.	Yes[6]	c.a. 100	Yes	> 100[10]	No
Voltri Massif	470	< 0.001[2]	N.d.	c.a. 200	Yes	>100[12]	No
Aosta Valley	225	N.d.	Yes[7]	c.a. −20	Yes	> 100[13]	No
Valmalenco	70	N.d.	Yes[8]	c.a. 100	Yes	> 100[14]	No
Ligurian-Emilian Apennines	110	0.04[3]	N.d.	c.a. 15	Yes	>100[12]	Yes
Tuscan Apennines	130	6.4[4]	N.d.	c.a. 0	Yes	>100[15]	Yes
Calabrian arc	45	< 0.0005[5]	N.d.	c.a. - 10	Yes	< 100[16]	Yes

N.d. = no data; 1) Structural Model of Italy at scale 1:500,000 (ISPRA); 2) [95]; 3) [99]; 4) [79]; 5) INGV dataset (see Table S2); 6) [113]; 7) [124]; 8) [125]; 9) Earth Magnetic Anomaly Grid-EMAG2v3; 10) Geological Map of Torino Ovest at scale 1: 50,000 (ISPRA); 11) [126]; 12) [111]; 13) [127]; 14) Geological Map of Valmalenco at scale 1:25,000, Montrasio et al., 2005; 15) [61]; 16) Brandt and Schenk, 2021.

and approximately 45 km^2 in Calabria (Table 4). Beyond H_2 emissions already discussed in the previous section, additional indicators of fossil serpentinization include: (i) measurements of H_2 trapped within fluid inclusions as evidence of past serpentinization events and (ii) magnetic anomalies as indirect evidence of serpentinite bodies at depth.

Micro-Raman spectroscopy performed on fluid inclusions within veins collected in serpentinite outcrops of the Lanzo Massifs, Aosta Valley, and Valmalenco reveals the occurrence of serpentinization-derived H_2 in brines [113,124,125,130]. A recent paleomagnetic investigation by Siravo et al. [126] in the Ivrea–Verbano Zone (IVZ) revealed a low to very low degree of serpentinization, consistent with limited magnetite formation. Conversely, aeromagnetic anomaly maps by Caratori Tondini et al. [131] and Meyer et al. [102]; EMAG2v3) display particularly high magnetic anomalies (>100 nT) in correspondence with the Lanzo and Voltri massifs, suggesting the presence of large serpentinite bodies at shallow depths (<4 km).

To date, no studies have documented H_2 trapping within fluid inclusions in the Apennines. Considering magnetic anomalies, Donzé et al. [19] reported that ophiolites of the Northern Apennines display average anomalies of 11 nT weaker than those observed in analogous settings such as the H_2-rich chromite mine of Albania (above 20 nT). However, the lenticular geometry of serpentinite bodies in the Apennines enclosed within sedimentary successions likely attenuates or obscures regional magnetic signatures, explaining the relatively weak anomalies observed in these areas.

5.2.2. Conditions

In the Alpine domain, the Voltri Massifs, Lanzo Massif, Aosta Valley, and Valmalenco exhibit wide surface exposures of serpentinites, indicating extensive fossil serpentinization that, nowadays, likely continues at depth [62,108,111,127]. These ophiolites record multiple serpentinization episodes initially related to oceanic hydrothermal alteration and subsequently to subduction-related metamorphism (e.g., Ref. [113,124,130,132]). Multiple serpentinization phases linked to oceanic and subduction metamorphism [113,124,130,132], followed by exhumation, likely modified or partially disrupted the original lithological or structural architecture, suggesting that part of the H_2 generated during past serpentinization may have been lost [133]. The Ivrea–Verbano Zone, despite hosting deep peridotitic units, shows negligible serpentinization and only minor or negligible surface serpentinite [126], indicating minimal H_2 generation and little to no potential for fossil H_2 preservation.

In the Apennine domain, the Ligurian–Emilian, Tuscan, and Calabrian ophiolites record Jurassic serpentinization of Alpine Tethys ultramafic rocks (ca. 150 Ma; [119]). Serpentinites in these regions form ultramafic lenses enclosed within rocks of contrasting permeability, such as pelitic or carbonate formations [134,135]. Although discontinuous and fragmentary, the geometry of these serpentinite lenses—volumetrically significant, particularly in the Tuscan Apennines [61,134]—provides favorable conditions for H_2 preservation.

Overall, in the Alpine domain, most of the H_2 produced during past serpentinization was likely lost as a result of the erosion of sedimentary cover during the orogen building, limiting the preservation of ancient reservoirs. In contrast, the Apennine ophiolites retain the geological and structural prerequisites for economically attractive H_2 preservation.

5.3. Hydrothermal alteration of iron-rich intrusive and volcanic rocks

5.3.1. Evidence

Biotite-rich granitoids and metagranitoids, emplaced during the late stages of the Hercynian orogeny and later overprinted by Alpine deformation and, locally, metamorphism, are widely exposed across the Western, Central, and Southern Alps (~7000 km^2) (e.g., Ref. [136]). Several Alpine-age granitic plutons, including the Adamello (~675 km^2), Bergell (~250 km^2), and Biella (~40 km^2), were emplaced in the surroundings of the Insubric Line about 30 Ma ago ([137–139]; Fig. 5). These intrusions are notably biotite-rich (13–20 vol%), particularly in the Adamello pluton [140]. Limited soil-gas measurements near these granitoids detected minor H_2 of likely biological rather than abiotic origin [93]. In Sardinia, late Hercynian granitoids (~300 Ma) cover ~5500 km^2 and contain 5–30 vol% magnesium-rich biotite. However, such a composition is less favorable for H_2 generation ([141]; Table 5), as testified by low H_2 (0.02 vol%) concentrations detected in thermal springs (Table 5 and S2). In the Calabria–Peloritani Arc (~3500 km^2), Hercynian granitoids affected by Alpine metamorphism and post-orogenic extension show intense biotite alteration (up to 27 vol %) to clay minerals and Fe-oxides, potentially producing H_2, though only trace amounts have been detected in surface fluid surveys (Table 5 and S2). Trace H_2 concentrations detected in Sardinian and Calabrian granitoids are associated with crustal $^3He/^4He$ signatures (R/Ra_c between 0.3 and 0.02; see Table S2), suggesting an abiotic origin. Additionally, recent granitoid intrusions (~90 km^2), emplaced between 8.4 and 5 Ma in the Tuscan Archipelago (Elba, Montecristo, Giglio) and less than 5 Ma in mainland Tuscany (Montecatini, Gavorrano, Campiglia) [69,143], are enriched in Fe-biotite (5-10 vol%) [144,145]. Despite their small outcrop extent, these granitoid intrusions are characterized by larger subsurface volumes overlained by low-permeability metamorphic units [146,147], creating favorable conditions for hydrogen traps. Extensional faulting promotes the interaction between these plutons and hydrothermal fluids, leading to widespread replacement of Fe-biotite by phlogopite, chlorite, and titanite [145,148]. Geochemical analyses of hydrothermal fluids from the Larderello geothermal region show significant concentrations of H_2 (Table 5 and S3), associated with CH_4 and CO_2 exhibiting abiotic isotopic signatures [78,82].

5.3.2. Conditions

The volumetric cut-off for Fe-rich granitoid bodies is widely exceeded across all investigated regions due to the large subsurface extent of these plutons (Table 5). However, high heat flow and active hydrothermal circulation are essential for H_2 generation via biotite alteration. In this framework, Tuscany stands out for its exceptionally high heat flow—up to 400 mW/m^2—exploited in the Larderello geothermal field above a granitoid intrusion 6–23 km wide and exceeding 20,000 km^3 in volume [69,142,149]. Although Leila et al. [78] attributed the H_2 detected at Larderello to serpentinization, hydrothermal alteration of biotite-rich granitoids remains a plausible source, as shown by the Fe-biotite to Fe-chlorite transformation observed in analogous Tuscan granites [145,150]. Elsewhere, granitoid regions show normal geothermal gradients (~30 °C/km) and moderate heat flow (<100 mW/m^2), confining hydrothermal reactions to depths that are economically unfeasible (Figs. 5 and 6). Nonetheless, structural evidence indicates generally favorable settings for gas migration and localized entrapment. Low-temperature weathering of Fe-rich granitoids may further contribute to H_2 generation [51], implying that ancient plutonic complexes in the Alps, Sardinia, and Calabria could act as long-term, low-grade H_2 sources.

5.4. H_2-GR3: organic-rich rocks

5.4.1. Evidence

The H2-GR3 group comprises organic matter-rich rocks (coal, shale, and bituminous carbonates). In Italy, exploitable coal reserves are generally absent with the exception of the Sulcis Basin, which contains both mineable and deeper (i.e., at 1-2.5 km of depth) coal seams [151]. Italy is the most hydrocarbon-endowed country in southern Europe, with discovered reserves of 1840 million barrels of oil and about 30 trillion ft^3 of gas. Roughly 75% of Italian oil production comes from the Val d'Agri field (Southern Apennines), while most gas production occurs in the Adriatic foreland [152].

Major kerogen-rich source rocks in Italy are thrust-related, folded Mesozoic carbonates such as the Villafortuna–Trecate and Gaiano (Po Basin), Val d'Agri (Southern Apennines), and Gela (Sicily) hydrocarbon reservoirs. Two other important source rock types are: (1) Oligo-Miocene shales deposited in the foredeep wedges of the Southern Alps and the Apennines (e.g., Cortemaggiore, Luna, and Gagliano fields), which form small gas accumulations; and Plio-Pleistocene turbidites

Table 5
Evidence and conditions for hydrothermal alteration of granites in target areas indicating whether each selected areas satisfies the ranking criteria defined in the semi-quantitative H_2 Prospectivity Index framework (Appendix A and Table S3).

Target area	Evidence			Conditions				
	Target rock exposure (Fe-rich granitoids) (km^2)[1]	Alkaline springs	H_2 emissions (vol %)	Target rocks at depth (Fe-rich granitoids)	Volume estimates (km^3)	Heat flow (mW/m^2)[5]	Active magmatic/hydrothermal system	Favorable structural architecture
Alps	7000	N.d.	N.d.	Yes	> 100	40-70	No	Yes
Sardinia	5500	No	<0.05[2]	Yes	> 100	50-90	No	Yes
Calabrian-Peloritani arc	3500	No	<0.0001[2]	Yes	> 100	50	Yes	Yes
Tuscany	90	Yes	6.4[3]	Yes	> 100[4]	400	Yes	Yes

N.d. = no data; Data from: 1) Geological Map of Italy at 1:1,000,000 scale (ISPRA); 2) update [85] dataset (see Table S2); 3) [79]; 4) [142]; 5) [103].

deposited in late Apennine foredeeps (Po Basin and Adriatic Sea), which are biogenic gas sources [152].

Low H_2 concentrations (<0.01 vol%) together with abiotic CH_4 and $^3He/^4He$ ratios indicating mixing between crustal and mantle components (i.e., R/Ra_c between 0.45 and 1.3) have been measured across these regions enclosing organic-rich rocks ([85,153]; see also Figs. 5 and 6 and Table S1–S2).

5.4.2. Conditions

Due to the difficulty of estimating the volume of organic matter-rich rocks, recent works recommend focusing on total organic carbon (TOC) data [18,43]. Reporting a strong linear correlation between H_2 generation and TOC, Moretti et al. [43] demonstrated that rocks with TOC exceeding 40 wt%, such as those in the Sulcis and Po basins, exhibit significant H_2 generation potential. H_2 -GR3 can generate H_2 under anoxic conditions through thermogenic dissociation of C–H bonds at high temperatures (≈200–600°C) during late thermal maturation via aromatization, polycondensation, or metathesis mechanisms [43,154,155]. Using paleotemperature indicators such as vitrinite reflectance (Ro, %), H_2 generation is inferred to initiate during the early maturity stage of kerogen ($R_o > 0.6\%$), accelerate under overmature conditions ($R_o > 1.5\%$), and reach a maximum generation rate at R_o values around 3.5% [155]. Kerogen-rich Mesozoic carbonates in Italy have generally experienced from middle to late maturity ($R_o\% > 0.7$; [156]), with maximum $R_o\%$ values of 1 in Sicily [157], 1.4 in the Val d'Agri Basin [158], and 3.3% in the Po Basin[159], the latter approaching the inferred H_2 yield peak [155]. By contrast, Sulcis coal and the organic-rich shales of the Adriatic foreland exhibit early mature and immature thermal stages, respectively ($R_o < 0.7\%$; [151,160]). In addition to high-temperature thermogenic processes, low-temperature (<200°C) oxidation of coal, due to its interaction with oxygen (usually air), can also produce significant amounts of H_2 (Wang et al., 2017; [43]). Consequently, the shallow coal seams of the Sulcis Basin, characterized by TOC values exceeding 40 wt%, could locally generate H_2, which, however, will easily escape into the air. Given Italy's dense well network, we recommend systematic monitoring of H_2 concentrations in organic-rich regions—particularly those at a late-maturity stage—to better quantify the national H_2 generation potential associated with organic matter.

6. Semi-quantitative synthesis of Italian hydrogen prospectivity

In the previous sections, both direct and indirect evidence of natural H_2 in Italy, as well as the main geological and thermal conditions controlling its generation and preservation, were qualitatively discussed (Tables 3–6). These analyses, performed for each geological process, provided the conceptual basis for a methodological transition: the conversion of descriptive parameters into weighted numerical indicators, subsequently integrated within a semi-quantitative assessment grid (Table S3). Based on H_2_index outcomes, we define distinct H_2 prospectivity classes, which range from high (>0.75) to moderate (0.5-0.7), low (0.25-0.5), and very low (<0.25).

In the case of active serpentinization, the highest scores are obtained for the Voltri ultramafic Massif, where the combination of significant peridotite volumes (both exposed and at depth) and the presence of hyperalkaline fluids ([94,95,97,98,116,117]; Fig. 5) results in a moderate potential (H_2_index ≈ 0.72; Moderate class; Table 7). The other ultramafic complexes of the Alps, the Lanzo Massif and the Ivrea–Verbano Zone, are characterized by a low prospectivity (H_2_index ≈ 0.43; Table 7), due to the lack of direct evidence (CF = 0.74) that reduces the final score. Future target hydrogeochemical analyses are critical to better constrain H_2 prospectivity in these regions. The Ligurian–Emilian Apennines, where hydrogeochemical data are available (CF = 1), display a moderate potential (H_2_index = 0.52) lower than the Voltri Massif, due to the limited occurrence of fresh peridotite at depth. Overall, active serpentinization in Italy could occur in Alpine ultramafic complexes under relatively low-temperature conditions, allowing H_2 generation but with low efficiency (Table 3 and S3).

The H_2_index increases when fossil serpentinization systems are considered. In this context, serpentinites of the Northern Apennines show higher prospectivity (H_2_index ≈ 0.83; High class; Table 7) than those of Voltri, Lanzo, Valmalenco, and Aosta Valley (H_2-index ≈ 0.51 to 0.63; Moderate class; Table 7), reflecting the more favorable structural configuration of the Apennines that potentially allows the long-term preservation of H_2 generated in the past.

Our H_2_index calculation reveals that the most significant contribution in absolute terms derives from hydrothermal alteration of Fe-rich intrusive rocks, which represent the highest Italian potential for H_2 exploration. The Tuscany region is characterized by an H_2_index of 1.00 (High class; Table 7), supported by direct evidence of H_2 emissions (up to 6 vol% in fumarolic gases), extremely high heat flow (>400 mW m^{-2}), and the presence of still-hot Fe-bearing granitic intrusions (Larderello, Mt. Amiata). The Alps, Sardinia, and Calabria display moderate to low values (H_2_index ≈ 0.46–0.60; Table 7), consistent with the presence of extensive Fe-rich granitoids and favorable lithologies but cooler present-day thermal regimes and limited H_2 emissions. In these regions, natural hydrogen generation appears possible but subdued.

Thermogenic degradation of organic matter exhibits high prospectivity in the Po Basin due to the high concentration of Total Organic Compounds (TOC) and the late mature thermal stage (H_2_index ≈ 0.77; Table 7), as indicated by data available for the Gaiano Field.

Overall, the semi-quantitative synthesis outlines a dual prospectivity pattern for Italy (Fig. 7). Tuscany stands out as the most favorable area under active conditions, representing a natural laboratory for investigating hydrogen generation associated with hydrothermal alteration of Fe-rich granitoids. The Voltri Massifs show a good balance between evidence and geological conditions, combining active and fossil potential, whereas the Ligurian–Emilian-Tuscan Apennines are a good target for preserved reservoirs of H_2 derived from past serpentinization events. The Po Basin is a target area to investigate the potential preservation of H_2 produced from the thermogenic degradation of the organic matter.

Table 6
Evidence and conditions for thermogenic degradation of organic matter in target areas, indicating whether each selected area satisfies the ranking criteria defined in the semi-quantitative H_2 Prospectivity Index framework (Appendix A and Table S3).

Target area	Evidence		Conditions			
	H_2 emissions (vol %)	Hydrocarbon wells[6]	Target rocks at depth (organic matter-rich rocks)	Total Organic Compounds (wt%)	Thermal maturity (R_o %)	Favorable structural architecture
Sulcis Basin	<0.0002[1]	No	Yes	46[7]	0.7[7]	No
Po Basin	<0.015[2]	Yes	Yes	12 to 46[8]	0.4-3.3[8]	Yes
Val d'Agri Basin	<0.007[3]	Yes	Yes	5[9]	0.6-1.4[11]	Yes
Adriatic foreland	< 0.0002[4]	Yes	Yes	1 to 6[10]	0.2-0.6[10]	Yes
Sicily	< 0.0001[5]	Yes	Yes	1 to 14.5[8]	0.6-1[12]	Yes

1) [161]; 2) [153]; 3) INGV database (see Table S2); 4) [88]; 5) [162]; 6) MASE database [101]; 7) [151]; 8) [159]; 9) [163]; 10) [160]; 11) [158]; 12) [157].

Table 7
Summary of hydrogen prospectivity classes in Italy.

Process	Target area	Completeness Factor (CF)	H_2_index	Prospectivity class
GR1a – Active serpentinization	Voltri Massif	1	0.72	Moderate
	Ligurian–Emilian Apennines	1	0.52	Moderate
	Ivrea–Verbano Zone (IVZ)	0.74	0.43	Low
	Lanzo Massif	0.74	0.43	Low
GR1b – Fossil serpentinization	Ligurian–Emilian-Tuscan Apennines	0.91	0.83	High
	Lanzo Massif	0.91	0.63	Moderate
	Valmalenco	0.91	0.63	Moderate
	Voltri Massif	0.91	0.55	Moderate
	Aosta Valley	0.91	0.51	Moderate
	Calabrian Apennines	0.91	0.39	Low
GR2 – hydrothermal alteration of Fe-rich intrusive rocks	Tuscany	1	1	High
	Calabrian–Peloritani Arc	1	0.60	Moderate
	Sardinia	1	0.60	Moderate
	Alps	0.77	0.46	Low
GR3 – Thermogenic degradation of organic matter	Po Basin	1	0.77	High
	Adriatic Foreland	1	0.42	Low
	Val d'Agri	1	0.42	Low
	Sicilian fields	1	0.42	Low
	Sulcis Basin	1	0.34	Low

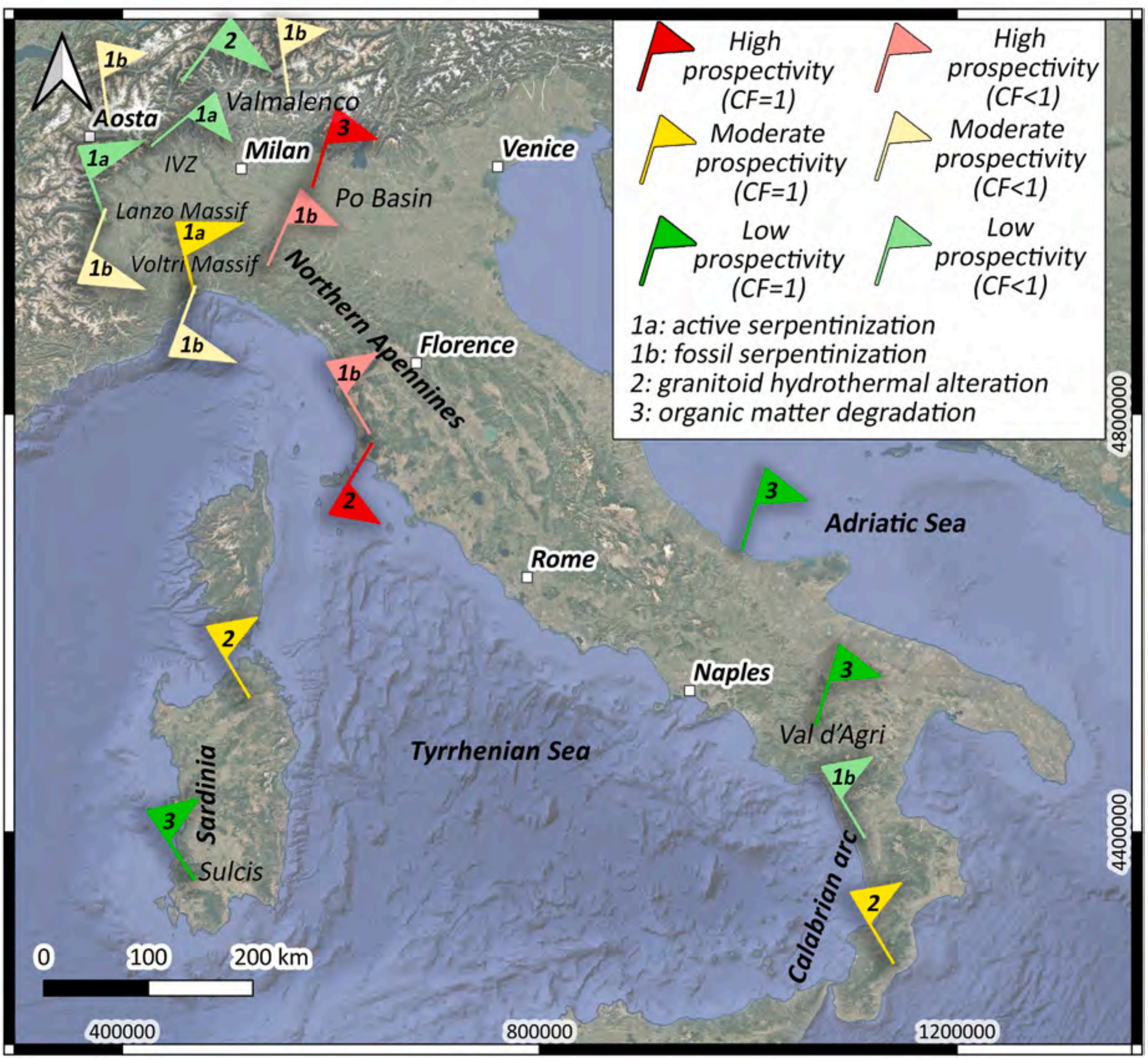

Fig. 7. The summary map of target area prioritization for hydrogen exploration. CF = completeness factor.

Moreover, the large Alpine ultramafic massifs (Lanzo, Voltri, and Ivrea–Verbano) as well as Fe-rich plutons of the Alps, Sardinia, and Calabria define promising contexts to better understand H_2 production from low-temperature oxidation of Fe^{2+}-bearing secondary minerals (e.

g., magnetite, serpentinite, and chlorite).

7. Robustness and implementation of the semi-quantitative approach

The proposed workflow has been calibrated on well-known areas in Italy, where it was possible to verify the internal consistency among modelled scores. Specifically, areas with higher H_2_index values correspond to regions where all or most indicators are favorable for hydrogen potential (e.g., the Northern Apennines and the Tuscan geothermal region, which exhibit both the highest value of H_2_index and the most elevated H_2 concentrations in shallow fluids; see Table S3). In contrast, areas with lower H_2_index values correspond to regions where H_2 generation is geologically impossible or highly unlikely (e.g., the Calabrian arc and the Ivrea Verbano Zone, which show the lowest H_2_index values due to the absence of suitable volumes of source rocks at depth; see Table S3). These results confirm the robustness and reliability of the proposed approach.

This study represents an initial pre-exploration step toward identifying H_2-producing systems. As new systems are discovered and the understanding of natural hydrogen systems improves, the model can be further constrained through enhanced calibration and the integration of newly available geological evidence/assessment criteria, thereby supporting the progressive refinement of target prioritization over time.

8. Conclusions

This study introduces a novel pre-exploration workflow that integrates conceptual geological knowledge with weighted, reaction-specific evidence and condition indicators to obtain a numerical H_2_index that quantifies exploration prospectivity. By enabling spatial prioritization of areas where conditions for, primarily, H_2 generation and, secondarily, preservation coexist, this framework provides a robust and transferable tool for sustainable subsurface H_2 exploration consistent with the UN 2030 Agenda (SDG 7).

Applied to Italy—where no national-scale H_2 prospectivity assessment previously existed—the workflow highlights significant and spatially diverse potential. Over 30,000 km^2 of exposed rocks were identified as suitable H_2 sources, including ≈8000 km^2 of ultramafic complexes with potential H_2 derived from active or fossil serpentinization and ≈22,000 km^2 of Fe-rich igneous bodies with hydrothermal reduction potential. Widespread hydrocarbon systems further indicate buried organic matter capable of thermogenic H_2 generation. This spatially resolved analysis reveals the potential coexistence of active generation zones and fossil reservoirs. This distinction is critical, as it implies fundamental differences in the type and scale of the required exploration strategies. Active serpentinization systems represent a continuous and potentially renewable process, whereas fossil reservoirs rely on structural and stratigraphic trapping conditions capable of preserving H_2 over geological timescales.

Primary exploration targets identified by the semi-quantitative workflow include: (1) Tuscany, the top-priority region combining large granitoid volumes with active hydrothermal activity; (2) the Voltri Massif, with favorable conditions for both active and fossil serpentinization; (3) the Ligurian, Emilian, and Tuscan serpentinites, offering strong preservation potential for fossil H_2; (4) the Po Basin, which could preserve H_2 generated from the thermogenic degradation of organic matter; and (5) the Ivrea–Verbano and Lanzo ultramafic rocks, together with the granitoids of Calabria, Sardinia, and the Western and Central Alps, ideal settings for studying H_2 generation under low-temperature secondary oxidation reactions.

Rather than a single, dominant hydrogen province, Italy's prospectivity is distributed across a network of localized opportunities controlled by distinct lithological, thermal, and tectonic factors. From an operational perspective, two priority actions emerge for advancing exploration in these target areas.

- Expand geochemical analysis of both shallow, especially across ultramafic complexes in the Alps and Northern Apennines, and deep fluids, exploiting the dense well network of Italy.
- Develop high-resolution 3D geological models to delineate reactive rock volumes and identify potential traps.

Our national-scale synthesis converts complex geological constraints into decision-ready insights that de-risk early decisions, optimize allocation of capital and field efforts, and support scenario planning. The proposed semi-quantitative workflow is transferable to other regions, contributing to the global energy transition by integrating natural hydrogen into broader decarbonization strategies alongside geothermal resources and existing gas infrastructures.

Declaration of generative AI and AI-assisted technologies in the manuscript preparation process

During the preparation of this work, the author(s) used ChatGPT to improve the clarity, grammar, and style of the English text. After using this tool, the authors reviewed and edited the content as needed and take full responsibility for the content of the published article.

CRediT authorship contribution statement

G. Schirripa Spagnolo: Conceptualization, Data curation, Formal analysis, Investigation, Methodology, Validation, Visualization, Writing – original draft, Writing – review & editing. **I. Baneschi:** Formal analysis, Methodology, Validation, Writing – review & editing. **A. Rielli:** Validation, Writing – review & editing. **A. Billi:** Validation, Writing – review & editing. **A.C. Ogunyele:** Investigation, Writing – review & editing. **L. Aldega:** Validation, Writing – review & editing. **M. Lelli:** Investigation, Validation, Writing – review & editing. **A. Caracausi:** Investigation, Validation, Writing – review & editing. **L. Smeraglia:** Validation, Writing – review & editing. **G.M. Riolo:** Investigation, Writing – review & editing. **A. Correale:** Validation, Writing – review & editing. **E. Carminati:** Conceptualization, Funding acquisition, Investigation, Methodology, Project administration, Resources, Supervision, Validation, Visualization, Writing – original draft, Writing – review & editing. **C. Boschi:** Conceptualization, Data curation, Formal analysis, Funding acquisition, Investigation, Methodology, Project administration, Resources, Supervision, Validation, Visualization, Writing – original draft, Writing – review & editing.

Declaration of competing interest

The authors declare the following financial interests/personal relationships which may be considered as potential competing interests: Chiara Boschi reports financial support was provided by Italian Ministry of University and Research. If there are other authors, they declare that they have no known competing financial interests or personal relationships that could have appeared to influence the work reported in this paper.

Acknowledgments

This article was developed as part of the Natural Hydrogen for Energy trAnsiTion project (NHEAT project, https://www.nheat-project.it), funded by the Italian Ministry of University and Research (MUR) through the PRIN 2022 PNRR programme. The authors express their gratitude for this support, which has been pivotal in advancing research on natural hydrogen resources in Italy. The authors would also like to thank Andrea Dini for helpful discussions as well as Laurent Truche, Isabelle Moretti, and three anonymous reviewers for their valuable advice, which contributed to improving this work.

Appendix A. Supplementary data

Supplementary data to this article can be found online at https://doi.org/10.1016/j.ijhydene.2026.156933.

References

[1] European Commission. The European Green Deal (COM(2019) 640 final). 2019. Brussels. Last visit 11/11/2025, https://eur-lex.europa.eu/legal-content/EN/TXT/?uri=CELEX:52019DC0640.

[2] European Commission. REPowerEU Plan (COM(2022) 230 final). Brussels. Last visit 11/11/2025, https://eur-lex.europa.eu/legal-content/EN/TXT/?uri=CELEX:52022DC0230; 2022.

[3] International Energy Agency (IEA). Global Hydrogen Review 2023. Paris: OECD/IEA; 2023. Last visit 11/11/2025, https://www.iea.org/reports/global-hydrogen-review-2023.

[4] International Renewable Energy Agency (IRENA). Global hydrogen trade to meet the 1.5°C climate goal: green hydrogen cost and potential. Abu Dhabi: IRENA; 2022. Last visit 11/11/2025, https://www.irena.org/Publications/2022/May/Global-hydrogen-trade-Cost.

[5] Musa M, Hosseini T, Sander R, Frery E, Sayyafzadeh M, Haque N, Kinaev N. Techno-economic assessment of natural hydrogen produced from subsurface geologic accumulations. Int J Hydrogen Energy 2024;93:1283–94. https://doi.org/10.1016/j.ijhydene.2024.11.009.

[6] Singh CH. The emergence of natural hydrogen: genesis and current perspectives. Scientific Contributions Oil and Gas 2025;48(1):91–112. https://doi.org/10.29017/scog.v48i1.1691.

[7] Zhang K, Ma X, Zheng B, Jin Z. Techno-economic viability of natural hydrogen. Natl Sci Rev 2025;12(10). https://doi.org/10.1093/nsr/nwaf368. nwaf368.

[8] European Hydrogen Observatory. Hydrogen basics factsheets: hydrogen value chains. Last visit 11/11/2025, https://observatory.clean-hydrogen.europa.eu/learn-about-hydrogen/hydrogen-basics/hydrogen-value-chains; 2023.

[9] Wong K, Cascone M, Giovannelli D, Vitale Brovarone A. Formation and fluxes of natural hydrogen in the crust and upper mantle. Earth-Sci Rev 2026;275:105400. https://doi.org/10.1016/j.earscirev.2026.105400.

[10] Jackson O, Lawrence SR, Hutchinson IP, Stocks AE, Barnicoat AC, Powney M. Natural hydrogen: sources, systems and exploration plays. Geoenergy 2024;2(1). https://doi.org/10.1144/geoenergy2024-002. geoenergy2024-002.

[11] Ellis GS, Gelman SE. Model predictions of global geologic hydrogen resources. Sci Adv 2024;10. https://doi.org/10.1126/sciadv.ado0955. eado0955.

[12] Lodhia BH, Peeters L, Frery E. A review of the migration of hydrogen from the panetary to basin scale. J Geophys Res Solid Earth 2024;129(6):e2024JB028715. https://doi.org/10.1029/2024jb028715.

[13] Nicoletti L, Hidalgo JC, Strąpoć D, Moretti I. H2 transport in sedimentary bsin. Geosciences 2025;15(8):298. https://doi.org/10.3390/geosciences15080298.

[14] Etiope G, Ellis GS, Ardakani OH, Boreham CJ, Klitzke P, Martín-Monge A, Reis HLS, Templeton AS, Soo Kim H, Gaucher E, Sissmann O. Understanding the resource potential of natural hydrogen on Earth: scientific gaps, uncertainties and recommendations. Earth Sci Rev 2026:105413. https://doi.org/10.1016/j.earscirev.2026.105413.

[15] Maiga O, Deville E, Laval J, Prinzhofer A, Diallo AB. Characterization of the spontaneously recharging natural hydrogen reservoirs of Bourakebougou in Mali. Sci Rep 2023;13(1):11876. https://doi.org/10.1038/s41598-023-38977-y.

[16] Truche L, Donzé F-V, Goskolli E, Muceku B, Loisy C, Monnin C, Dutoit H, Cerepi A. A deep reservoir for hydrogen drives intense degassing in the Bulqizë ophiolite. Science 2024;383:618–21. https://doi.org/10.1126/science.adk9099.

[17] Moretti I, Brouilly E, Loiseau K, Prinzhofer A, Deville E. Hydrogen emanations in intracratonic areas: new guidelines for early exploration basin screening. Geosci 2021;11:145. https://doi.org/10.3390/geosciences11030145.

[18] Lévy D, Boka-Mene M, Meshi A, Fejza I, Guermont T, Hauville B, Pelissier N. Looking for natural hydrogen in Albania and Kosova. Front Earth Sci 2023;11:1167634. https://doi.org/10.3389/feart.2023.1167634.

[19] Donzé F-V, Lefeuvre N, Truche L, Yao Y, Vujević I, Dutoit H. Natural hydrogen exploration within Western European and eastern Mediterranean ophiolites and ultramafic complexes. Geochem Explor Environ Anal 2024;24(4). https://doi.org/10.1144/geochem2024-043. geochem2024-043.

[20] Neal C, Stanger G. Hydrogen generation from mantle source rocks in Oman. Earth Planet Sci Lett 1983;66:315–20. https://doi.org/10.1016/0012-821X(83)90144-9.

[21] Truche L, Joubert G, Dargent M, Martz P, Cathelineau M, Rigaudier T, Quirt D. Clay minerals trap hydrogen in the Earth's crust: evidence from the Cigar Lake uranium deposit, Athabasca. Earth Planet Sci Lett 2018;493:186–97. https://doi.org/10.1016/j.epsl.2018.04.038.

[22] Klein F, Tarnas JD, Bach W. Abiotic sources of molecular hydrogen on Earth. Elements 2020;16:19–24. https://doi.org/10.2138/gselements.16.1.19.

[23] Zgonnik V. The occurrence and geoscience of natural hydrogen: a comprehensive review. Earth Sci Rev 2020;203:103140. https://doi.org/10.1016/j.earscirev.2020.103140.

[24] Milkov AV. Molecular hydrogen in surface and subsurface natural gases: Abundance, origins and ideas for deliberate exploration. Earth Sci Rev 2022;230:104063. https://doi.org/10.1016/j.earscirev.2022.104063.

[25] Ballentine CJ, Karolytė R, Cheng A, Sherwood Lollar B, Gluyas JG, Daly MC. Natural hydrogen resource accumulation in the continental crust. Nat Rev Earth Environ 2025;6:342–56. https://doi.org/10.1038/s43017-025-00670-1.

[26] Moretti I, Prinzhofer A, Ammouial J, Bouton N. Natural hydrogen generation from Phanerozoic sedimentary siderite. Minerals 2025;15(11):1218. https://doi.org/10.3390/min15111218.

[27] Tanelli G, Benvenuti M, Costagliola P, Dini A, Lattanzi P, Maineri C, Mascaro I, Ruggieri G. The iron mineral deposits of Elba island: state of the art. Ofioliti 2001;26:239–48. https://doi.org/10.4454/ofioliti.v26i2a.148.

[28] Martin S, Toffolo L, Moroni M, Montorfano C, Secco L, Agnini C, Nimis P, Tumiati S. Siderite deposits in northern Italy: early Permian to Early Triassic hydrothermalism in the Southern Alps. Lithos 2017;284:276–95. https://doi.org/10.1016/j.lithos.2017.04.002.

[29] Lin L-H, Slater GF, Lollar B, Lacrampe-Couloume G, Onstott TC. The yield and isotopic composition of radiolytic H_2, a potential energy source for the deep subsurface biosphere. Geochem Cosmochim Acta 2005;69:893–903. https://doi.org/10.1016/j.gca.2004.07.032.

[30] Warr O, Giunta T, Ballentine CJ, Lollar BS. Mechanisms and rates of ^{4}He, ^{40}Ar, and H_2 production and accumulation in fracture fluids in Precambrian Shield environments. Chem Geol 2019;530:119322. https://doi.org/10.1016/j.chemgeo.2019.119322.

[31] Dini A, Rocchi S, Westerman DS, Pertusati P. Microchemical and textural evolution of accessory minerals in the Capo Bianco aplite–pegmatite dike (Elba Island, Italy): constraints on late-stage magmatic and post-magmatic evolution. Lithos 2004;75(1–2):35–66. https://doi.org/10.1016/j.lithos.2003.12.016.

[32] Callegari I, Bezzon GP, Broggini C, Buso GP, Caciolli A, Carmignani L, Colonna T, Fiorentini H, Guastaldi E, Xhixha MK, Mantovani F, Massa G, Menegazzo R, Mou L, Pirro A, Rossi Alvarez C, Strati V, Xhixha G, Zanon A. Total natural radioactivity, Tuscany, Italy. J Maps 2013;9(3):438–43. https://doi.org/10.1080/17445647.2013.802999.

[33] Caridi F, Di Bella M, Sabatino G, Belmusto G, Fede MR, Romano D, Italiano F, Mottese AF. Assessment of natural radioactivity and radiological risks in River sediments from Calabria (Southern Italy). Appl Sci 2021;11:1729. https://doi.org/10.3390/app11041729.

[34] Fuchs YA. Hydrothermal alteration at the Novazza volcanic field and its relation to the u–mo–zn Novazza deposit, northern Italy. In: Metallogenesis of uranium deposits. IAEA tech. Comm. Meeting, Vienna, 9–12 March 1987; 1989. p. 137–48.

[35] Nascimben P. Studio sulla distribuzione dell'uranio nelle ligniti di alcuni giacimenti italiani. CNEN-RT/GEO-70-7. Roma: Comitato Nazionale per l'Energia Nucleare; 1970. p. 27.

[36] McCollom TM, Bach W. Thermodynamic constraints on hydrogen generation during serpentinization of ultramafic rocks. Geochem Cosmochim Acta 2009;73(3):856–75. https://doi.org/10.1016/j.gca.2008.10.032.

[37] Vacquand C, Deville E, Beaumont V, Guyot F, Sissmann O, Pillot D, Arcilla C, Prinzhofer A. Reduced gas seepages in ophiolitic complexes: evidences for multiple origins of the H_2–CH_4–N_2 gas mixtures. Geochem Cosmochim Acta 2018;223:437–61. https://doi.org/10.1016/j.gca.2017.12.018.

[38] Potter J, Rankin AH, Treloar PJ. Abiogenic Fischer–Tropsch synthesis of hydrocarbons in alkaline igneous rocks; fluid inclusion, textural and isotopic evidence from the Lovozero complex, N.W. Russia. Lithos 2004;75(3–4):311–30. https://doi.org/10.1016/j.lithos.2004.03.003.

[39] Murray J, Clément A, Fritz B, Schmittbuhl J, Bordmann V, Fleury JM. Abiotic hydrogen generation from biotite-rich granite: a case study of the Soultz-sous-Forêts geothermal site, France. Appl Geochem 2020;119:104631. https://doi.org/10.1016/j.apgeochem.2020.104631.

[40] Truche L, Bourdelle F, Salvi S, Lefeuvre N, Zug A, Lloret E. Hydrogen generation during hydrothermal alteration of peralkaline granite. Geochem Cosmochim Acta 2021;308:42–59. https://doi.org/10.1016/j.gca.2021.05.048.

[41] Arrouvel C, Prinzhofer A. Genesis of natural hydrogen: new insights from thermodynamic simulations. Int J Hydrogen Energy 2021;46(36):18780–94. https://doi.org/10.1016/j.ijhydene.2021.03.057.

[42] Mahlstedt N, Horsfield B, Weniger P, Misch D, Shi X, Noah M, Boreham C. Molecular hydrogen from organic sources in geological systems. J Nat Gas Sci Eng 2022;105:104704. https://doi.org/10.1016/j.jngse.2022.104704.

[43] Moretti I, Bouton N, Ammouial J, Carrillo A. The H_2 potential of the Colombian coals in natural conditions. Int J Hydrogen Energy 2024;77:1443–56. https://doi.org/10.1016/j.ijhydene.2024.06.225.

[44] Gilat A, Vol A. Primordial hydrogen–helium degassing: an overlooked major energy source for internal terrestrial processes. HAIT J Sci Eng 2005;B 2(1–2):125–67.

[45] Peccerillo A. Plio-Quaternary volcanism in Italy: petrology, geochemistry, geodynamics. Berlin: Springer; 2005.

[46] Früh-Green GL, Connolly JAD, Kelley DS, Plas A, Grobety B. Serpentinization of oceanic peridotites: implications for geochemical cycles and biological activity. In: Wilcock WD, et al., editors. The subseafloor biosphere at mid-ocean ridges. Geophys. Monogr. Ser., vol. 144. Washington, D.C: AGU; 2004. p. 119–36.

[47] Evans BW, Hattori K, Baronnet A. Serpentinite: what, why, where? Elements 2013;9(2):99–106. https://doi.org/10.2113/gselements.9.2.99.

[48] Klein F, Bach W, McCollom TM. Compositional controls on hydrogen generation during serpentinization of ultramafic rocks. Lithos 2013;178:55–69. https://doi.org/10.1016/j.lithos.2013.03.008.

[49] Schwarzenbach EM, Vogel M, Früh-Green GL, Boschi C. Serpentinization, carbonation, and metasomatism of ultramafic sequences in the Northern Apennine ophiolite (NW Italy). J Geophys Res Solid Earth 2021;126(5). https://doi.org/10.1029/2020JB020619. e2020JB020619.

[50] McCollom TM, Seewald JS. Serpentinites, hydrogen, and life. Elements 2013;9(2):129–34. https://doi.org/10.2113/gselements.9.2.129.

[51] Geymond U, Briolet T, Combaudon V, Sissmann O, Martinez I, Duttine M, Moretti I. Reassessing the role of magnetite during natural hydrogen generation. Front Earth Sci 2023;11:1169356. https://doi.org/10.3389/feart.2023.1169356.
[52] Hutchinson IP, Jackson O, Stocks AE, Barnicoat AC, Lawrence SR. Greenstones as a source of hydrogen in cratonic sedimentary basins. Geol Soc London Spec Publ 2024;547:511–25. https://doi.org/10.1144/SP547-2023-39.
[53] Bourdet J, Delle Piane C, Wilske C, Mallants D, Suckow A, Questiaux D, Gerber C, Crane P, Deslandes A, Martin L, Aleshin M. Natural hydrogen in low temperature geofluids in a Precambrian granite, South Australia. Implications for hydrogen generation and movement in the upper crust. Chem Geol 2023;638:121698. https://doi.org/10.1016/j.chemgeo.2023.121698.
[54] Gregory SP, Barnett MJ, Field LP, Milodowski AE. Subsurface microbial hydrogen cycling: natural occurrence and implications for industry. Microorganisms 2019; 7:53. https://doi.org/10.3390/microorganisms7020053.
[55] Dal Piaz GV, Bistacchi A, Massironi M. Geological outline of the Alps. Episodes 2003;26(3):175–80. https://doi.org/10.18814/epiiugs/2003/v26i3/004.
[56] Vai GB. Basement and early (pre-Alpine) history. In: Anatomy of an orogen: the Apennines and adjacent Mediterranean basins. Netherlands, Dordrecht: Springer; 2001. p. 121–50.
[57] ISPRA Geological Map of Italy at scale 1:1,000,000. Last visit 11/11/2025, https://sgi.isprambiente.it/milione/milione5ed.html.
[58] Gaggero L, Crispini L, Isola E, Marescotti P. Asbestos in natural and anthropic ophiolitic environments: a case study of geohazards related to the Northern Apennine ophiolites (Eastern Liguria, Italy). Ofioliti 2013;38(1):29–40. https://doi.org/10.4454/ofioliti.v38i1.414.
[59] Boschi C, Dini A, Baneschi I, Bedini F, Perchiazzi N, Cavallo A. Brucite-driven CO_2 uptake in serpentinized dunites (Ligurian Ophiolites, Montecastelli, Tuscany). Lithos 2017;288–289:264–81. https://doi.org/10.1016/j.lithos.2017.07.005.
[60] Rizzo G, Buccione R, Dichicco MC, Punturo R, Mongelli G. Petrography, geochemistry and mineralogy of serpentinite rocks exploited in the ophiolite units at the Calabria–Basilicata boundary, southern Apennine (Italy). Fibers 2023;11 (10):81. https://doi.org/10.3390/fib11100081.
[61] Dini A, Rielli A, Di Giuseppe P, Ruggieri G, Boschi C. The ophiolite-hosted Cu–Zn VMS deposits of Tuscany (Italy). Minerals 2024;14:273. https://doi.org/10.3390/min14030273.
[62] Scambelluri M, Philippot P. Deep fluids in subduction zones. Lithos 2001;55(1–4): 213–27. https://doi.org/10.1016/S0024-4937(00)00046-3.
[63] Hattori K, Guillot S. Geochemical character of serpentinites associated with high- to ultrahigh-pressure metamorphic rocks in the Alps, Cuba, and the Himalayas: recycling of elements in subduction zones. G-cubed 2007;8(9):Q09010. https://doi.org/10.1029/2007GC001594.
[64] Schaltegger U, Corfu F. The age and source of late Hercynian magmatism in the central Alps: evidence from precise U−Pb ages and initial Hf isotopes. Contrib Mineral Petrol 1992;111:329–44. https://doi.org/10.1007/BF00311195.
[65] Rottura A, Bargossi GM, Caironi V, Del Moro A, Maccarrone E, Macera P, Paglionico A, Petrini R, Piccareta G, Poli G. Petrogenesis of contrasting Hercynian granitoids from the Calabrian Arc, southern Italy. Lithos 1990;24:97–119. https://doi.org/10.1016/0024-4937(90)90019-W.
[66] Carmignani L, Carosi R, Di Pisa A, Gattiglio M, Musumeci G, Oggiano G, Pertusati PC. The Hercynian chain in Sardinia (Italy). Geodin. Acta 1994;7(1): 31–47. https://doi.org/10.1080/09853111.1994.11105257.
[67] Venturelli G, Thorpe RS, Dal Piaz GV, Del Moro A, Potts PJ. Petrogenesis of calc-alkaline, shoshonitic and associated ultrapotassic Oligocene volcanic rocks from the Northwestern Alps, Italy. Contrib Mineral Petrol 1984;86:209–20. https://doi.org/10.1007/BF00373666.
[68] Carminati E, Lustrino M, Doglioni C. Geodynamic evolution of the central and western Mediterranean: tectonics vs. igneous petrology constraints. Tectonophysics 2012;579:173–92. https://doi.org/10.1016/j.tecto.2012.01.026.
[69] Dini A, Gianelli G, Puxeddu M, Ruggieri G. Origin and evolution of Pliocene–Pleistocene granites from the Larderello geothermal field (Tuscan Magmatic Province, Italy). Lithos 2005;81(1–4):1–31. https://doi.org/10.1016/j.lithos.2004.09.002.
[70] Acocella V, Rossetti F. The role of extensional tectonics at different crustal levels on granite ascent and emplacement: an example from Tuscany (Italy). Tectonophysics 2002;354:71–83. https://doi.org/10.1016/S0040-1951(02)00290-1.
[71] Farina F, Stevens G, Dini A, Rocchi S. Peritectic phase entrainment and magma mixing in the late Miocene Elba Island laccolith–pluton–dyke complex (Italy). Lithos 2012;153:243–60. https://doi.org/10.1016/j.lithos.2012.05.011.
[72] Lustrino M, Wilson M. The circum-Mediterranean anorogenic Cenozoic igneous province. Earth Sci Rev 2007;81(1–2):1–65. https://doi.org/10.1016/j.earscirev.2006.09.002.
[73] Lustrino M, Morra V, Fedele L, Franciosi L. Beginning of the apennine subduction system in central western Mediterranean: constraints from Cenozoic "orogenic" magmatic activity of Sardinia, Italy. Tectonics 2009;28(5). https://doi.org/10.1029/2008TC002419.
[74] Peccerillo A. Multiple mantle metasomatism in central-southern Italy: geochemical effects, timing and geodynamic implications. Geology 1999;27: 315–8. https://doi.org/10.1130/0091-7613(1999)027%3C0315:MMMICS%3E2.3.CO;2.
[75] Chiodini G, Cardellini C, Amato A, Boschi E, Caliro S, Frondini F, Ventura G. Carbon dioxide Earth degassing and seismogenesis in central and southern Italy. Geophys Res Lett 2004;31:L07615. https://doi.org/10.1029/2004GL019480.
[76] Buttitta D, Capasso G, Paternoster M, Barberio MD, Gori F, Petitta M, Picozzi M, Caracausi A. Regulation of deep carbon degassing by gas-rock-water interactions in a seismic region of Southern Italy. Sci Total Environ 2023;897:165367. https://doi.org/10.1016/j.scitotenv.2023.165367.
[77] Caracausi A, Italiano F, Paonita A, Rizzo A, Nuccio PM. Evidence of deep magma degassing and ascent by geochemistry of peripheral gas emission at mt. Etna (Italy): assessment to the magmatic reservoir pressure. J Geophys Res 2003;108 (B10):2463. https://doi.org/10.1029/2002JB002095.
[78] Leila M, Lévy D, Battani A, Piccardi L, Šegvić B, Badurina L, Pasquet G, Combaudon V, Moretti I. Origin of continuous hydrogen flux in gas manifestations at the Larderello geothermal field, Central Italy. Chem Geol 2021; 585:120564. https://doi.org/10.1016/j.chemgeo.2021.120564.
[79] Granieri D, Mazzarini F, Cerminara M, Calusi B, Scozzari A, Menichini M, Lelli M. Shallow portion of an active geothermal system revealed by multidisciplinary studies: the case of Le Biancane (Larderello, Italy). Geothermics 2023;108: 102616. https://doi.org/10.1016/j.geothermics.2022.102616.
[80] Tedesco D, Allard P, Sano Y, Wakita H, Pece R. Helium-3 in subaerial and submarine fumaroles of Campi Flegrei caldera, Italy. Geochem Cosmochim Acta 1990;54(4):1105–16. https://doi.org/10.1016/0016-7037(90)90442-N.
[81] Inguaggiato S, Pecoraino G, D'Amore F. Chemical and isotopical characterisation of fluid manifestations of Ischia Island (Italy). J Volcanol Geoth Res 2000;99: 151–78. https://doi.org/10.1016/S0377-0273(00)00158-X.
[82] Tassi F, Fiebig J, Vaselli O, Nocentini M. Origins of methane discharging from volcanic, hydrothermal and cold emissions in Italy. Chem Geol 2012;310–311: 36–48. https://doi.org/10.1016/j.chemgeo.2012.03.018.
[83] Duchi V, Campana ME, Minissale A, Thompson M. Geochemistry of thermal fluids on the volcanic isle of Pantelleria, southern Italy. Appl Geochem 1994;9:147–60. https://doi.org/10.1016/0883-2927(94)90004-3.
[84] Minissale A, Evans WC, Magro G, Vaselli O. Multiple source components in gas manifestations from north-central Italy. Chem Geol 1997;142(3–4):175–92. https://doi.org/10.1016/s0009-2541(97)00081-8.
[85] Minissale A, Donato A, Procesi M, Pizzino L, Giammanco S. Systematic review of geochemical data from thermal springs, gas vents and fumaroles of southern Italy for geothermal favourability mapping. Earth Sci Rev 2019;188:514–35. https://doi.org/10.1016/j.earscirev.2018.09.008.
[86] Etiope G, Klusman RW. Geologic emissions of methane to the atmosphere. Chemosphere 2002;49:777–89. https://doi.org/10.1016/S0045-6535(02)00380-6.
[87] Minissale A, Magro G, Martinelli G, Vaselli O, Tassi GF. Fluid geochemical transect in the Northern Apennines (central-northern Italy): fluid genesis and migration and tectonic implications. Tectonophysics 2000;319:199–222. https://doi.org/10.1016/S0040-1951(00)00031-7.
[88] Minissale A. Origin, transport and discharge of CO_2 in central Italy. Earth Sci Rev 2004;66:89–141. https://doi.org/10.1016/j.earscirev.2003.09.001.
[89] Paternoster M, Oggiano G, Sinisi R, Caracausi A, Mongelli G. Geochemistry of two contrasting deep fluids in the Sardinia microplate (western Mediterranean): relationships with tertiary tectonics and volcanism. J Volcanol Geoth Res 2017; 336:108–17. https://doi.org/10.1016/j.jvolgeores.2017.02.011.
[90] Chiodini G, Cioni R. Gas geobarometry for hydrothermal systems and its application to some Italian geothermal areas. Appl Geochem 1989;4:465–72. https://doi.org/10.1016/0883-2927(89)90004-8.
[91] Minissale A, Vaselli O, Tassi F, Magro G, Grechi GP. Fluid mixing in carbonate aquifers near Rapolano (central Italy): chemical and isotopic constraints. Appl Geochem 2002;17:1329–42. https://doi.org/10.1016/S0883-2927(02)00023-9.
[92] Gherardi F, Panichi C, Gonfiantini R, Magro G, Scandiffio G. Isotope systematics of C-bearing gas compounds in the geothermal fluids of Larderello, Italy. Geothermics 2005;34(4):442–70. https://doi.org/10.1016/j.geothermics.2004.09.005.
[93] Etiope G, Ciotoli G, Benà E, Mazzoli C, Röckmann T, Sivan M, Squartini A, Laemmel T, Szidat S, Haghipour N, Sassi R. Surprising concentrations of hydrogen and non-geological methane and carbon dioxide in the soil. Sci Total Environ 2024;948:174890. https://doi.org/10.1016/j.scitotenv.2024.174890.
[94] Brozzo G, Marini L, Prochilo F, Zuccolini MV. Atlante degli acquiferi della Liguria — volume IV: l'acquifero alluvionale della bassa valle del Fiume Magra. Pisa: Pacini Editore; 2009.
[95] Boschetti T, Etiope G, Pennisi M, Romain M, Toscani L. Boron, lithium and methane isotope composition of hyperalkaline waters (Northern Apennines, Italy): terrestrial serpentinization or mixing with brine? Appl Geochem 2013;32: 17–25. https://doi.org/10.1016/j.apgeochem.2012.08.018.
[96] Boschetti T, Manzi V, Toscani L. Ca/Mg and Ca/Sr ratios in salt water from Messinian sedimentary basins: tracing diagenetic effects and paleo-seawater composition. Aquat Geochem 2013;19:195–208. https://doi.org/10.1007/s10498-013-9186-7.
[97] Chavagnac V, Monnin C, Ceuleneer G, Boulart C, Hoareau G. Characterization of hyperalkaline fluids produced by low-temperature serpentinization of mantle peridotites in the Oman and Ligurian ophiolites. G-cubed 2013;14:2496–522. https://doi.org/10.1002/ggge.20147.
[98] Schwarzenbach EM, Lang SQ, Früh-Green GL, Lilley MD, Bernasconi SM, Méhay S. Sources and cycling of carbon in continental, serpentinite-hosted alkaline springs in the Voltri Massif, Italy. Lithos 2013;177:226–44. https://doi.org/10.1016/j.lithos.2013.07.009.
[99] De Freitas VA, Montanini A, Moretti I, Artoni A, Segadelli S, Izerumugaba JP, Battani A, Etiope G. Geological and geochemical approach to natural hydrogen exploration in the Northern Apennines, Italy. Mar Petrol Geol 2025;182:107594. https://doi.org/10.1016/j.marpetgeo.2025.107594.
[100] MASE Geological Map of Italy at scale 1:500,000. http://wms.pcn.minambiente.it/ogc?map=/ms_ogc/WMS_v1.3/Vettoriali/Carta_geologica.map&service=wms&request=getCapabilities&version=1.3.0.

[101] MASE database. Last visit 11/11/2025, https://unmig.mase.gov.it/ricerca-e-coltivazione-di-idrocarburi/pozzi-produttivi/.
[102] Meyer B, Chulliat A, Saltus R. Derivation and Error Analysis of the Earth Magnetic Anomaly Grid at 2 arc min Resolution Version 3 (EMAG2v3). G-cubed 2017;18:4522–37. https://doi.org/10.1002/2017GC007280.
[103] Della Vedova B, Bellani S, Pellis G, Squarci P. Deep temperatures and surfaceheat flow density distribution. In: Vai GB, Martini P, editors. Anatomy of anOrogen: the apennines and adjacent Mediterranean basins. Dordrecht, Netherlands: Kluwer Academic Publishers; 2001. p. 65–76.
[104] Leong JA, Nielsen M, McQueen N, Karolytė R, Hillegonds DJ, Ballentine C, Darrah T, McGillis W, Kelemen P. H_2 and CH_4 outgassing rates in the Samail ophiolite, Oman: implications for low-temperature, continental serpentinization rates. Geochem Cosmochim Acta 2023;347:1–15. https://doi.org/10.1016/j.gca.2023.02.008.
[105] Hydrogen Europe. Clean hydrogen production pathways report 2024. 2024. Brussels. Last visit 11/11/2025, https://hydrogeneurope.eu/wp-content/uploads/2024/06/2024_H2E_CleanH2ProductionPathwaysReport.pdf.
[106] European Commission. Hydrogen. Directorate-General for energy, Brussels. 2025. Last visit 11/11/2025, https://energy.ec.europa.eu/topics/eus-energy-system/hydrogen_en.
[107] Granieri D, Chiodini G, Avino R, Caliro S. Carbon dioxide emission and heat release estimation for Pantelleria Island (Sicily, Italy). J Volcanol Geoth Res 2014;275:22–33. https://doi.org/10.1016/j.jvolgeores.2014.02.011.
[108] Schmid SM, Kissling E. The arc of the western Alps in the light of geophysical data on deep crustal structure. Tectonics 2000;19:62–85. https://doi.org/10.1029/1999TC900057.
[109] Scarponi M, Kvapil J, Plomerová J, Solarino S, Hetényi G. New constraints on the shear-wave velocity structure of the Ivrea geophysical body from seismic ambient noise tomography (Ivrea-Verbano Zone, Alps). Geophys J Int 2024;236:1089–105. https://doi.org/10.1093/gji/ggad470.
[110] De Freitas VA, Boschetti T, Moretti I, Montanini A. Hydrogen generation potential of peridotites and pyroxenites in ophiolitic settings. Chem Geol 2026:123266. https://doi.org/10.1016/j.chemgeo.2026.123266.
[111] Molli G, Crispini L, Malusà M, Mosca P, Piana F, Federico L. Geology of the Western Alps-Northern Apennines junction area: a regional review. In: Beltrando M, editor. The geology of Italy, journal of the virtual explorer. Electronic Edition, 36 2010. paper 9. Download from. http://virtualexplorer.com.au/article/2009/215/apennine-alps.
[112] Piccardo GB. The Lanzo peridotite massif, Italian Western Alps: jurassic rifting of the Ligurian Tethys. Geol Soc London Spec Publ 2010;337:47–69. https://doi.org/10.1144/SP337.3.
[113] Vitale Brovarone A, Martinez I, Elmaleh A, et al. Massive production of abiotic methane during subduction evidenced in metamorphosed ophicarbonates from the Italian Alps. Nat Commun 2017;8:14134. https://doi.org/10.1038/ncomms14134.
[114] Malatesta C, Crispini L, Federico L, Capponi G, Scambelluri M. The exhumation of high-pressure ophiolites (Voltri Massif, Western Alps): insights from structural and petrologic data on metagabbro bodies. Tectonophysics 2012;568:102–23. https://doi.org/10.1016/j.tecto.2011.08.024.
[115] Tribuzio R, Thirlwall MF, Vannucci R. Origin of the gabbro–peridotite association from the Northern Apennine ophiolites (Italy). J Petrol 2004;45(6):1109–24. https://doi.org/10.1093/petrology/egh006.
[116] Marini L, Ottonello G. Atlante degli acquiferi della Liguria, vol. 3: le acque dei complessi ofiolitici (bacini: Arrestra, Branega, Cassinelle, Cerusa, Erro, Gorzente, Leira, Lemme, Lerone, Orba, Piota, Polcevera, Rumaro, Sansobbia, Stura, Teiro, Varenna, Visone). Università degli Studi di Genova, Pacini, Pisa. 2002.
[117] Cipolli F, Gambardella B, Marini L, Ottonello G, Vetuschi Zuccolini M. Geochemistry of high-pH waters from serpentinites of the Gruppo di Voltri (Genova, Italy) and reaction path modeling of CO_2 sequestration in serpentinite aquifers. Appl Geochem 2004;19(5):787–802. https://doi.org/10.1016/j.apgeochem.2003.10.007.
[118] Ryberg T, Haberland C, Wawerzinek B, Stiller M, Bauer K, Zanetti A, Ziberna L, Hetényi G, Müntener O, Weber MM, Krawczyk CM. 3-D imaging of the Balmuccia peridotite body (Ivrea–Verbano Zone, NW Italy) using controlled source seismic data. Geophys J Int 2023;234(3):1985–98. https://doi.org/10.1093/gji/ggad182.
[119] Marroni M, Meneghini F, Pandolfi L. From accretion to exhumation in a fossil accretionary wedge: a case history from the Gottero Unit (Northern Apennines, Italy). Geodin. Acta 2004;17:41–53. https://doi.org/10.3166/ga.17.41-53.
[120] Macdonald AH, Fyfe WS. Rate of serpentinization in seafloor environments. Tectonophysics 1985;116:123–35. https://doi.org/10.1016/0040-1951(85)90225-2.
[121] Berndt ME, Allen DE, Seyfried WE. Reduction of CO_2 during serpentinization of olivine at 300 °C and 500 bar. Geology 1996;24(4):351–4. https://doi.org/10.1130/0091-7613(1996)024<0351:ROCDSO>2.3.CO;2.
[122] Malvoisin B, Brunet F, Carlut J, Rouméjon S, Cannat M. Serpentinization of oceanic peridotites: 2. Kinetics and processes of San Carlos olivine hydrothermal alteration. J Geophys Res 2012;117:B04102. https://doi.org/10.1029/2011JB008842.
[123] Chavagnac V, Ceuleneer G, Monnin C, Lansac B, Hoareau G, Boulart C. Mineralogical assemblages forming at hyperalkaline warm springs hosted on ultramafic rocks: a case study of Oman and Ligurian ophiolites. G-cubed 2013;14(7). https://doi.org/10.1002/ggge.20146.
[124] Ferrando S, Frezzotti ML, Orione P, Conte RC, Compagnoni R. Late-Alpine rodingitization in the Bellecombe meta-ophiolites (Aosta Valley, Italian Western Alps): evidence from mineral assemblages and serpentinization-derived H_2-bearing brine. Int Geol Rev 2010;52(10–12):1220–43. https://doi.org/10.1080/00206810903557761.
[125] Peretti A, Dubessy J, Mullis J, Frost BR, Trommsdorff V. Highly reducing conditions during Alpine metamorphism of the Malenco peridotite (Sondrio, northern Italy) indicated by mineral paragenesis and H2 in fluid inclusions. Contrib Mineral Petrol 1992;112:329–40. https://doi.org/10.1007/BF00310464. 1992.
[126] Siravo G, Speranza F, Minelli L, Zucali M, Fazio E, Caricchi C, Spagnuolo L. Magnetic and paleomagnetic characterization of the Ivrea-Verbano lower crust body (NW Italy): assessing the magnetization of variscan-age lower crust. J Geophys Res Solid Earth 2025;130(6). https://doi.org/10.1029/2024JB031017. e2024JB031017.
[127] Ellero A, Loprieno A. Nappe stack of Piemonte–Ligurian units south of Aosta Valley: new evidence from Urtier Valley (Western Alps). Geol J 2017;53:1665–84. https://doi.org/10.1002/gj.2984.
[128] Debret B, Nicollet C, Andreani M, Schwartz S, Godard M. Three steps of serpentinization in an eclogitized oceanic serpentinization front (Lanzo Massif–Western Alps). J Metamorph Geol 2013;31(2):165–86. https://doi.org/10.1111/jmg.12008.
[129] Fornasaro S, Comodi P, Crispini L, Malatesta C, Zucchini A, Marescotti P. Potentially toxic elements distribution in the serpentinized and deformed ultramafic rocks from the Voltri Massif (NW, Italy). Period Mineral 2019;88:259–76. https://doi.org/10.2451/2019PM874.
[130] Giuntoli F, Menegon L, Siron G, Cognigni F, Leroux H, Compagnoni R, Rossi M, Vitale Brovarone A. Methane-hydrogen-rich fluid migration may trigger seismic failure in subduction zones at forearc depths. Nat Commun 2024;15:480. https://doi.org/10.1038/s41467-023-44641-w. 2024.
[131] Caratori Tontini F, Stefanelli P, Giori I, Faggioni O, Carmisciano C. The revised aeromagnetic anomaly map of Italy. Ann Geophys 2004;47(5). https://doi.org/10.4401/ag-3358.
[132] Scambelluri M, Müntener O, Hermann J, Piccardo GB, Trommsdorff V. Subduction of water into the mantle: history of an Alpine peridotite. Geology 1995;23(5):459–62. https://doi.org/10.1130/0091-7613(1995)023<0459:SOWITM>2.3.CO;2.
[133] Pjang S, Mouthereau F, Robert A, Kumar A, Callot JP. A petro-physical model for Serpentinized mantle and origin of natural hydrogen in the pyrenees. G-cubed 2025;26. https://doi.org/10.1029/2024GC011804. e2024GC011804.
[134] Nirta G, Pandeli E, Principi G, Bertini G, Cipriani N. The Ligurian units of southern tuscany. Boll Soc Geol Ital 2005;3:29–54.
[135] Rielli A, Boschi C, Dini A. Tectonically driven carbonation of serpentinite by mantle CO_2: genesis of the Castiglioncello magnesite deposit in the Ligurian ophiolite of central Tuscany (Italy). Ore Geol Rev 2022;149:105022. https://doi.org/10.1016/j.oregeorev.2022.105022.
[136] Romer R, Schärer U, Steck A. Alpine and pre-alpine magmatism in the root-zone of the western Central Alps. Contrib Mineral Petrol 1996;123:138–58. https://doi.org/10.1007/s004100050147.
[137] Schaltegger U, Brack P, Ovtcharova M, Peytcheva I, Schoene B, Stracke A, Marocchi M, Bargossi GM. Zircon and titanite recording 1.5 million years of magma accretion, crystallization and initial cooling in a composite pluton (southern Adamello batholith, northern Italy). Earth Planet Sci Lett 2009;286:208–18. https://doi.org/10.1016/j.epsl.2009.06.028.
[138] Berger A, Thomsen TB, Ovtcharova M, Kapferer N, Mercolli I. Dating emplacement and evolution of the orogenic magmatism in the internal Western Alps: 1. The Miagliano Pluton. Swiss J Geosci 2012;105:49–65. https://doi.org/10.1007/s00015-012-0091-7.
[139] Gianola O, Schmidt MW, von Quadt A, Peytcheva I, Luraschi P, Reusser E. Continuity in geochemistry and time of the Tertiary Bergell intrusion (Central Alps). Swiss J Geosci 2014;107:197–222. https://doi.org/10.1007/s00015-014-0174-8.
[140] Grocolas T, Müntener O. The role of peritectic biotite for the chemical and mechanical differentiation of felsic plutonic rocks (Western Adamello, Italy). J Petrol 2024;65. https://doi.org/10.1093/petrology/egae009. egae009.
[141] Barbey P, Gasquet D, Pin C, Bourgeix AL. Igneous banding, schlieren and mafic enclaves in calc-alkaline granites: the Budduso pluton (Sardinia). Lithos 2008;104:147–63. https://doi.org/10.1016/j.lithos.2007.12.004.
[142] Gianelli G, Manzella A, Puxeddu M. Crustal models of the geothermal areas of southern Tuscany (Italy). Tectonophysics 1997;281(3–4):221–39. https://doi.org/10.1016/S0040-1951(97)00101-7.
[143] Dini A, Westerman DS, Innocenti F, Rocchi S. Magma emplacement in a transfer zone: the Miocene mafic Orano dyke swarm of Elba Island, 302. Tuscany, Italy: Geological Society, London, Special Publications; 2008. p. 131–48. https://doi.org/10.1144/SP302.10.
[144] Farina F, Dini A, Innocenti F, Rocchi S, Westerman DS. Rapid incremental assembly of the Monte Capanne pluton (Elba Island, Tuscany) by downward stacking of magma sheets. Bulletin 2010;122(9–10):1463–79. https://doi.org/10.1130/B30112.1.
[145] Paoli G, Dini A, Rocchi S. Footprints of element mobility during metasomatism linked to a late Miocene peraluminous granite intruding a carbonate host (Campiglia Marittima, Tuscany). Int J Earth Sci 2019;108(5):1617–41. https://doi.org/10.1007/s00531-019-01723-9.
[146] Bertini G, Casini M, Gianelli G, Pandeli E. Geological structure of a long-living geothermal system, Larderello, Italy. Terra Nova 2006;18(3):163–9. https://doi.org/10.1111/j.1365-3121.2006.00676.x.
[147] Vezzoni S, Rocchi S, Dini A. Lateral extrusion of a thermally weakened pluton overburden (Campiglia Marittima, Tuscany). Int J Earth Sci 2018;107(4):1343–55. https://doi.org/10.1007/s00531-017-1539-9.

[148] Villa IM, Ruggieri G, Puxeddu M, Bertini G. Geochronology and isotope transport systematics in a subsurface granite from the Larderello–Travale geothermal system (Italy). J Volcanol Geoth Res 2006;152(1–2):20–50. https://doi.org/10.1016/j.jvolgeores.2005.09.011.
[149] Minissale A. The Larderello geothermal field – a review. Earth Sci Rev 1991;31(2):133–51. https://doi.org/10.1016/0012-8252(91)90018-B.
[150] Boyce AJ, Fulignati P, Sbrana A. Deep hydrothermal circulation in a granite intrusion beneath Larderello geothermal area (Italy): constraints from mineralogy, fluid inclusions and stable isotopes. J Volcanol Geoth Res 2003;126(3–4):243–62.
[151] Plaisant A, Cara R, Multineddu D. Studio preliminare per l'applicazione di tecniche ECBM nel bacino carbonifero del Sulcis. 2009. Report RSE/2009/151.
[152] Bertello F, Fantoni R, Franciosi R, Gatti V, Ghielmi M, Pugliese A. From thrust-and-fold belt to foreland: hydrocarbon occurrences in Italy. https://doi.org/10.1144/0070113; 2010.
[153] Martinelli G, Dadomo A, Italiano F, Petrini R, Slejko FF. Geochemical monitoring of the 2012 Po Valley seismic sequence: a review and update. Chem Geol 2017:147–62. https://doi.org/10.1016/j.chemgeo.2016.12.013.
[154] Li X, Krooss BM, Weniger P, Littke R. Liberation of molecular hydrogen (H_2) and methane (CH_4) during non-isothermal pyrolysis of shales and coals: systematics and quantification. Int J Coal Geol 2015;137:152–64. https://doi.org/10.1016/j.coal.2014.11.011.
[155] Horsfield B, Mahlstedt N, Weniger P, Misch D, Vranjes-Wessely S, Han S, Wang C. Molecular hydrogen from organic sources in the deep Songliao Basin, PR China. Int J Hydrogen Energy 2022;47(38):16750–74. https://doi.org/10.1016/j.ijhydene.2022.02.208.
[156] Wu Y, Xia Y, Wang Y, Lei T, Liu Y, Liu Y, Hou X, Wang Y. The geochemical characteristics of coals from the Junggar Basin in Northwest China and the relation of the configuration of pristane with maturity in highly mature and over-mature samples. Oil & Gas Science and Technology–Revue d'IFP Energies nouvelles 2016;71(3):35. https://doi.org/10.2516/ogst/2015026.
[157] Caldarelli C, Smith D. Hydrocarbon systems in the onshore and offshore sicilian fold and thrust belt: new constraints from geochemical data. In: AAPG international conference and exhibition, Milan, Italy, October, vol. 23; 2011, October. p. 26.
[158] Noguera AM, Rea G. Deep structure of the campanian–lucanian arc (southern Apennine, Italy). Tectonophysics 2000;324(4):239–65. https://doi.org/10.1016/S0040-1951(00)00137-2.
[159] Katz BJ, Dittmar EI, Ehret GE. A geochemical review of carbonate source rocks in Italy. J Petrol Geol 2000;23(4):399–424. https://doi.org/10.1111/j.1747-5457.2000.tb00494.x.
[160] Cazzini F, Zotto OD, Fantoni R, Ghielmi M, Ronchi P, Scotti P. Oil and gas in the Adriatic foreland, Italy. J Petrol Geol 2015;38(3):255–79. https://doi.org/10.1111/jpg.12610.
[161] Minissale A, Magro G, Tassi F, Frau F, Vaselli O. The origin of natural gas emissions from Sardinia island, Italy. Geochem J 1999;33(1):1–12. https://doi.org/10.2343/geochemj.33.1.
[162] Favara R, Grassa F, Inguaggiato S, Valenza M. Hydrogeochemistry and stable isotopes of thermal springs: earthquake-related chemical changes along Belice Fault (Western Sicily). Appl Geochem 2001;16(1):1–17. https://doi.org/10.1016/S0883-2927(00)00015-9.
[163] Antoncecchi I. Modellazione geologico-strutturale 3D e sismicità indotta: il caso Val d'Agri. Italy: Earth Science Department of Sapienza University of Rome; 2020. PhD Thesis, https://iris.uniroma1.it/handle/11573/1623725.